UNIVERSITÀ DEGLI STUDI DI PALERMO
Dottorato di ricerca in Oncologia e Chirurgia Sperimentali
Dipartimento di Discipline Chirurgiche Oncologiche e Stomatologiche (Di.Chir.On.S.)

Doctor Europaeus

UNRAVELLING THE ROLES OF THE NUCLEAR PROTEIN NUPR1 DURING ER-STRESS INDUCTION.

Doctoral Dissertation of:
Dr. Angela Listì

Supervisor:
Prof. Juan Iovanna
Dr. Maria Teresa Borrello

Tutor:
Prof. Antonio Russo

The Chair of the Doctoral Program:
Prof. Antonio Russso

2019 – XXXII°

INDEX

Abstract

Background: NUPR1 was described as a transcriptional factor involved in the regulation of various cellular stress-response genes, playing a crucial role in the condition of the endoplasmic-reticulum (ER) stress, thus emerging as a common molecular factor of different pathologies, obesity, hepatic steatosis, and cancer.
In the present work we aim to explore how NUPR1 interacts with some pivotal genes that are the major modulators of the ER stress and metabolic cell functions. In particular we investigated the biochemical and molecular effects arising from the loss of NUPR1 in ER stress physiological conditions.
Methods: We used prolonged high fat diet (HFD) feeding to induce ER stress physiological in $Nupr1^{+/+}$ and $Nupr1^{-/-}$ male mice compared with their respectively normal chow diet (ND) controls. We fed mice with a HFD (60% fat, 20% protein, and 20% carbohydrate) for 10 weeks to promote chronic ER stress condition (Old-HFD group, *n*=5). An additional group of mice (*n*=5) was maintained on HFD (60% fat, 20% protein, and 20% carbohydrate) for a longer duration (15 weeks) to distinguish between age-dependent and age-independent effects.
Liver were collected for histological and molecular assessments. Western blots and RT-qPCR were performed to assess the expression levels of the major ER-stress response UPR-associated proteins and metabolic genes.
Results: We showed the downregulation of the majority of UPR-associated proteins: BIP ($p<0.0001$ for protein and mRNA), ATF4 ($p<0.0001$ for mRNA), XBP1 ($p<0.0001$ for protein and mRNA), CHOP ($p<0.0001$ for protein and mRNA), GADD34 (p=0.0296 for mRNA) in in-vivo $NUPR1^{-/-}$ compared to $NUPR1^{+/+}$ 10 weeks HFD mice. Western blot for the major UPR associated proteins in NURP1-/- mice at 15 weeks HFD showed similar expression trends reported at the time-point of 10 weeks. ERDj4 mRNA resulted down-regulated in $NUPR1^{-/-}$ compared to $NUPR1^{+/+}$ 15 weeks HFD mice (p=0.0032). Among the multiple metabolic genes, we reported a down-regulation of the majority mRNA associated to lipogenesis (SREBP, ACLY, ChREBP) and lipoprotein (APOB, PPAR-alfa, MTTP) in $NUPR1^{-/-}$ compared to $NUPR1^{+/+}$ HFD mice 15 weeks. Both LCAD and MCAD fatty acid metabolisms mRNA were also downregulated, as consequence of PPAR-alfa deficit. Similarly beta-oxidation mRNA ACOX1 and CPT1-alfa, as well as MTC4 and PGK1 were downregulated in $NUPR1^{-/-}$ compared to $NUPR1^{+/+}$ HFD mice 15 weeks.
Conclusion: The results of this work confirm that NUPR1 act downstream of the PERK branch playing a crucial role of NUPR1 in the activation of UPR response in physio-pathological ER stress condition and suggest a potential contribution of NUPR1-mediated ER stress response to the development of liver steatosis.

Summary

Considering the epidemic proportions of cancer, obesity and hepatic steatosis, there is an urgent need to better understand the cellular intrinsic molecular mechanism supporting these pathological conditions.
NUPR1 was described as a transcriptional factor involved in the regulation of various cellular stress-response genes, playing a crucial role in the condition of the endoplasmic-reticulum (ER) stress, thus emerging as a common molecular player of all such different pathologies. Although several evidences demonstrated that NUPR1 is able to activate several downstream genes in the UPR pathway, however the specific biological mechanisms underlying NUPR1 activity under ER stress conditions remains still to be established. For this reason we used prolonged high fat diet (HFD) feeding with the final aim of exploring the effect of Nupr1 loss in the ER stress in physiological conditions and characterize how NUPR1 interacts with some pivotal genes that are the major modulators of the ER stress and metabolic cell function. The results of our experiments showed that the loss of NUPR1 is associated to the downregulation of the majority of UPR-associated proteins (BIP, ATF4, XBP1, CHOP). These data confirm that NUPR1 act downstream of the PERK branch, playing a crucial role in the activation of UPR response in physio-pathological ER stress condition. To unraveling the potential role of NUPR1 in the development of liver steatosis, we decide to analyze also the transcriptomics profile of the major metabolic pathways genes. We reported a down-regulation of the majority mRNA associated to lipogenesis (SREBP, ACLY, ChREBP) and lipoprotein (APOB, PPAR-alfa, MTTP). These data suggest that an impaired UPR-mediated response, as observed in NUPR1 deficient mice, is associated to a reduced lipotoxocity, with a potential contribute of NUPR1-mediated ER stress response to the development of liver steatosis, which require further investigation in subsequent studies.

CHAPTER 1

Background, Rationale and Objectives

1.1 BACKGROUND

1.1.1 NUPR1

Nuclear Protein 1 (NUPR1), Candidate of Metastasis 1 (COM1), and P8 (OMIM: 614812) are the three alternative titles used to refer to the gene encoding an ubiquitous nuclear and cytoplasmic stress-activated protein.

Nupr1 is conserved from nematode to humans (1), has not a stable conformation, and analyzing its biophysical and biochemical characteristics, seems to have the same peculiarity of high-mobility group box proteins (HMG).(2) (3) By further investigations emerged the transcriptional role of this protein, the presence of helix-loop-helix binding (bHLH) domain (4) and the high affinity with the DNA, without preference of DNA sequence. Moreover in vitro experiments showed that the p8 phosphorylation might increase the DNA binding domain. (5) (6)

Nupr1 is able to act as transcriptional regulator of multiple genes, thanks to its peculiar interaction with the transcriptional p300/Smad cofactors complex. In vitro experiments showed that TGFbeta-1 activated p8 expression in cell-lines with P8 gene subjected to recombinant technologies. Inside a positive feedback, p8 enhanced the Smad-trans-activating, which was responsible for the TGFbeta-1 activity.(7) In the same years molecular biologists acquired additional tools to identify mechanisms evolutionarily preserved and responsible for the chromatin remodeling, including the relationship between p300 and Smad. (8). Subsequent pre-clinical studies on P8 protein clarify the potential association with p300 co-activator, showing as p300 might influence the regulation of glucagon genes' promoter activity by p8 involvement. (9)

Some systemic compounds, such as the Carbon tetrachloride (CCL_4) or the Lipopolysaccharides (LPS) induced the expression of NUPR1. CCl_4 is able to induce hepatic injury through several stages: necrosis, inflammatory infiltration, hepatic regeneration, cell proliferation, and deposition of connective tissue. Different experiments revealed that p8 sustained a protective effect in liver cells subjected to CCL_4 exposure. (10). Subsequently to the drug administration, the researchers observed a transient expression of P8 and a climax of p8 mRNA expression that returned at the basal level 48h after CCL4 injection. These data suggested a potential role of p8 as key transcriptional factor as well as strong and early partner in cell protective pathway. Similar data have been reported after LPS administration. Indeed a macroarray analysis performed on p8 $^{-/-}$ mice showed an improperly up- or down-regulation of several genes associated to the lack of p8, which could amplify the noxious consequences caused by this endotoxine. (11)

Among other experimental approaches designed to identify potential antitumoral or other healing effects of this protein, has been found that cannabinoides (12), glucose (13), angiotensine (14), vasoactive peptides such as endothelin-1 (ET-1) (15), and the transforming growth factor β-1 (TGFβ-1) (16) upregulated the p8 expression. The fast and transient activity of P8 in response to several stressors, certainly, do not make easy

to study this protein. Therefore several regulation mechanisms in which is implicated as well as the majority of potential partners remain still unclear.

The NUPR1 protein negatively regulates entosis through modulating AURKA activity. In pancreatic cancer, Iovanna et al., found a novel role for Nupr1, that, in the context of cell response to metabolic stress, favored cell survival by inhibiting autophagic cell death through *AURKA* expression.
They showed that, inducing silencing of Nupr1 expression or exposing pancreatic cancer cells to hypoxia or glucose starvation, several genes involved in the DNA repair and cell cycle were downregulated, inevitably assisting to the cell death, as result of DNA damage.
They showed also, that these situations increased when hypoxia or glucose starvation was combined with siNupr1 treatment, thus affirming that Nupr1 expression is activated in pancreatic cancer cells, as part of the response against metabolic stress. They found that *AUR*KA is one of the most interesting genes downregulated in response to metabolic stress and under the control of Nupr1.(17) A second work of the same researchers' team, showed that NUPR1-AURKA pathway counteracts the autophagy-dependent, CASP3-CASP7-independent cell death, induced by glucose starvation and hypoxia. Waiting for the development of molecular target inhibitors of NUPR1, the authors encouraged the use of AURKA inhibitors in tumors characterized by high NUPR1 expression. (18)

1.1.2 NUPR1 and Cancer

NUPR1 was first considered as a gene involved in the ER stress, primarily described as responsible of acute pancreatitis in rat pancreatic acinar cells. (2)
Few years later, Vasseur et al, cloned Nupr1, showing that 74% of the sequence was identical to the rat *P8* gene sequence, thus calling this protein as "P8". Subsequently they realized a multi tissue RNA blot with a human p8 clone probe at high stringency in order to identify which human tissues expressed the *P8* mRNA. In all tissues analyzed, a line of 0.80 kb for the p8 transcript was displayed, with some sensible difference of expression among different sites. Indeed an abundant expression has been detected in liver, pancreas, prostate, ovarian, colon, thyroid, spinal cord, trachea and adrenal gland, with moderate expression in heart, placenta, lung, skeletal muscle, kidney, testis, small intestine, stomach and lymph node, and low expression in brain, spleen, thymus and bone marrow. No expression has been noted in peripheral leukocytes. In the same work author suggested that p8 protein could be characterized by a bipartite domain for nuclear targeting. Indeed when COS-7, AR4-2J, HeLa cell lines were transfected by P8 containing plasmids, it acted as a promoter of cellular growth factors. (19)
In the same years (1999), Ree at al., who were exploring tumor cells metastatic processes, proclaimed the existence under the name of COM1 of a growth factor involved in breast cancer development.
In their work the authors explained the data obtained by comparing two molecular phenotypes. The first molecular profile was obtained from the bone marrow of a breast cancer patients. The second phenotype referred to cancer cells originated from bone marrow micro-metastasis of breast cancer patients, which, after stabilization in culture, were injected to generate "experimental metastasis" inside immune-deficient rats. The high expression of COM1 in the metastatic animal cells compared with the originally bone marrow breast cancer cells, led authors to sustain that this DNA-binding protein of HTH type, could mediate the growth response of tumor cells offered in a secondary target organ.
(20)
In a subsequent work of Ree A.H. et al., the evaluation of COM1 mRNA expressions was assessed in 81 samples of breast carcinoma tissues acquired from early step of clinical tumor progression and 27 respective non-neoplastic breast tissues. The significant higher expression of COM1 mRNA in breast cancer tissue could be

interpreted as the result of growth stimulatory signals coming from the tumor cells' stroma, thus suggesting that COM1 may contribute to the tumor aggressiveness phenotypes. In addition the authors showed that Com1 and p8 had the same sequence as well as the same gene's locus in chromosome 16 at position p11.2, which was often amplified in primary breast tumors, supporting p8 as growth promoting factor in the development of breast cancer. (21)

Further information about the potential role of NUPR1 in the early stage of cancer progression, come from studies conducted on mouse embryo fibroblasts (MEFs) taken from both $p8^{-/-}$ and $p8^{+/+}$ mouse genotypes. Both these cellular genotypes were transformed by retroviral vectors, including both *RAS* ^{V12} mutated and *E1A* oncogenes. As expected, the two original genotypes acted differently. Only transformed $p8^{+/+}$ MEFs formed colonies in soft agar, with tumor formation always reported in nude mice, after subcutaneously or intraperioneal injections of the transformed $p8^{+/+}$ MEFs. As control, when p8 expression was reprogrammed in transformed p8-/- MEFs, they may also generate tumor, confirming that P8 is critical for tumor development induced by ras ^{v12} mutated protein and the E1A oncongene. (22).

In 2012, T. Hamidi et al., according with the previous knowledge in this field of research , confirmed the role of NURP1 in promoting cancer disease.

Their work showed that the loss of Nurp1 was able to prevent the pancreatic intraepithelial neoplasms (PanINs) in mouse that constitutively expressed oncogenic Ras ^{G12D}.

The authors observed mouse models characterized by three different NURP1 genotypes, but all expressing *KRAS*^{G12D} mutation. As regards NURP1 gene, they had the following variants: (Nupr1-knockout) $NURP^{-/-}$; (Nupr1-omozygote) $NUPR1^{+/+}$; and (Nupr1-heterozygous)$NUPR1^{+/-}$. The period of observation ranged from 13 to 18 weeks. This experiment confirmed that Nurp1 played an essential role for the development of pancreatic cancer. Indeed all mouse *KRAS*^{G12D} $NUPR1^{+/+}$ at 13 week, only 3 of 9 *KRAS*^{G12D} NUPR1 $^{+/-}$ and none of *KRAS*^{G12D} NUPR1 $^{-/-}$ showed PanINs lesion.

To further explore the biological mechanisms of Nupr1 in cancer processes, the authors subjected pancreatic cancer cells to nutrient deprivation, as input to change their genes expression pattern, encouraging their survival ability after the induced stress. Transcriptomic studies were conducted to identify the genes affected after the siRNA-induced Nupr1 depletion, and both *RELB* and *IER3* genes were examined. *RELB* is a pro-survival gene of Nk-b family, while *IER3* is considered a *RELB* gene target, characterized by anti-apoptotic activity. Real time PCR and western blot suggested a significant association between the increase of the relative levels of *RELB* and the presence of Nupr1, which is able to bind the promoter of Nf-kB genes family, thus acting as their expression regulator. Further investigation about *RELB* and its regulator *NUPR1* reveled a positive feedback mechanism between them. Indeed measuring the level of *NURP1, RELB, IER3* mRNAs in a mouse model containing *KRAS*^{G12D} oncogene, authors reported an over-expression of all such three genes at week 8th, coinciding with the occurrence of the PanINs lesions. Another observation consisted in the diminished survival of pancreatic cancer cells without IER3, when subjected to nutrient deprivation. These evidences, along with additional data obtained blocking *IER3* expression alone or together with *NUPR1* or *RELB*, clearly suggested that these 3 factors acted through the same pathway.

Finally the authors tried to translate the results found in the mouse model in pancreatic ductal adenocarcinoma patients (PDAC). The tissues of 34 PDAC patients with a follow-up of 24 months were studied by immune-histochemistry assay and tissue microarray (TMA).

They reported an inverse correlation between Nupr1 expression and the time of survival. In addition a significant correlation of *NURP1, RELB, IER3* high expressions with the progression of PDAC suggested that they might be useful as a marker of poor prognosis. (23) .

In 2015, Grasso et al. confirmed Nupr1 like a chromatin binding protein responsible of the DNA methylation status, showing the relationships between NUPR1 protein and the activity of Dnmt1enzime, a specific DNA methylator that facilitates transformation required for oncogenic activation.
Using the ChIP assay demonstrated that Nupr1 binds to the *Dnmt1* promoter, revealing a direct effect of transcriptional regulation on this methylase enzyme.
By the luciferase based gene reporter assay in MiaPaCa2 cells transfected with siNupr1 or siControl they evidenced that the activation of the *Dnmt1* promoter decrease when Nupr1 was knockdown. Instead the overexpression of Nupr1 obtained in MiaPaCa2 cells by 100, 200 and 400 ng of pNupr1-Flag construct, increased *Dnmt1* promoter activity. They gained the same evidence in Panc1, a pancreatic cancer cells, confirming the involvement of Nupr1 expression in DNA methylation process.
The final evidence elucidating the molecular mechanism underlying the association of NUPR1 and DNMT1 downstream of Kras oncogene in the transformation of pancreas cells was obtained investigating the effect the DNA methyltransferase inhibitor 5-aza-2' -deoxycytydine (5-aza-dC).
At this point the authors planned to verify wether the drug-induced inhibition of DNA methylation could prevent the PanIN development in engeniereed mice.
They treated a Kras*G12D* expressing Nupr1+/+ mice with the 5-aza-dC, to reproduce the effect obtained when Nupr1is inactivated, demonstrating that the downregulation of Dnmt1 established the oncogene-induced senescence (OIS). As expected, the 5-aza-dC treatment reduced the development of PanINs lesions, confirming that the DNA methylation represents the crosstalk between NUPR1 and Kras oncogene transformation in pancreatic cancer. (24)

1.1.3 Endoplasmic Reticulum Stress

The endoplasmic reticulum (ER) is present in all eukariotic cells and plays a pivotal role in many processes of fundamental importance to guarantee cell survival in physiological cellular conditions. ER is the site of synthesis, folding and post-translational modifications of membrane and secreted proteins destined to the residence in ER and to the plasma membrane, or Golgi apparatus and lysosomes. (25). In addition the ER is involved in other cell vital processes, like the calcium homeostasis and lipid biosynthesis.
All this function are possible thanks to the peculiar architecture of the ER. Indeed this organelle is composed by a series of continuous membranes organized into sub-domains that include the rough-, smooth- , transitional-ER, and the nuclear envelope. The first researcher who saw these membranes full of polyribosomes, defined them like "rough" ER (RER). The RER is the site where the "protein synthesis" process began and the "Ca^{2+} signaling pathway" is regulated. The smooth ER is considered the major site of intracellular lipid biosynthesis, has a main role in Ca^{2+} signaling, and is also referred as the chief point of contact with other cellular organelles. (26)
The maturation of arising proteins in the endoplasmic reticulum is monitored by multiple disulfide-isomerases (PDI) that catalyze the formation of disulfide bridges by "molecular chaperones", a class of protein belonging to calcium-dependent families (such as GRP78, GRP94 and calreticulina), which prevent aggregation and allow their correct folding both in physiological and in pathological conditions. (27)
Protein folding is the process by which a linear polymer of amino-acids acquires the native conformation or rather a 3D structure capable of performing its cellular function. During this process, if the proteins required multiple attempts to obtain their conformation, they may be helped by the interaction with molecular chaperones that bind to the hydrophobic regions of unfolded proteins to facilitate the folding process. For this reason, the ER is considered like a quality control system able to ensure the correct folding and functions of the proteins until their final destination. Instead the misfolded or non-functioning proteins are retained in the ER and then, translocated in the cytosol for degradation by the 26S proteosome, a process mediated by the activation of the ER system Associated Degradation (ERAD).

Extracellular stimuli able to change intracellular homeostasis, including ER Ca2 +, glycosylation, energy stores, redox state, metabolic and inflammatory challenges, influenced the capacity of the ER folding, which results in the accumulation and aggregation of proteins that are not folded or badly folded and that began to accumulate inside the lumen of ER and generate a condition defined as stress of the endoplasmic reticulum. This protein's aggregates is toxic to cells and represents the biochemical basis of numerous physiopathological conditions associated with endoplasmic reticulum stress (ER stress) including cancer, metabolic diseases (insulin resistance, type 2 diabetes), neurodegenerative diseases (including Parkinson's, Alzheimer's, and Huntington's diseases) metabolic inflammation, cardiovascular diseases, viral infections and ophthalmology disorders (28). Melatonin and endoplasmic reticulum stress: relation to autophagy and apoptosis)

In order to avoid the deleterious effects associated to the ER stress, the cells evolved several protective strategies, called "Unfolded Protein Response" (UPR). The UPR aims to allow the elimination of misfolded proteins accumulated inside the ER favoring cellular survival with consequent restoration of the normal ER functioning (Schroder M, Kaufman RJ, 2005). However, if protein aggregation is persistent and the stress cannot be solved, UPR induces cell cycle arrest with subsequent apoptosis. This complex of cellular response is mediated by the activation of three trans-membrane receptors defined as stress sensors and respectively named: Pancreatic ER Kinase (PERK), Activating Transcription Factor 6 (ATF6) and Inositol-Requirng Enzyme 1 (IRE1α).

Although the exact molecular mechanism is not known, it appears that the reticular stress-induced apoptosis is mainly mediated by mitochondria and/or downstream activation of pro-apoptotic kinases dependent from the extrinsic apoptotic pathway, usually activated by the receptors of death. The hypothesis of a communication between ER and mitochondria is supported by experimental evidence that demonstrates the existence of a physical link between these two organelles (29). Indeed, structural and functional studies have revealed the existence of some contact areas between the ER membrane and the mitochondria membrane defined as Mitochondrial Associated Membranes (MAM), which play a critical role in the transmission of physiological and pathological signals from ER to mitochondria. Moreover, recent studies have shown that the induction of a persistent ER stress could represent a checkpoint in the regulation of the initiation phase of the mitochondria-mediated apoptotic pathway (30). Therefore, ER could be considered as the site where apoptotic signals are generated and integrated in order to induce cell death.

1.1.4 The UPR pathway

Under stressful situations, the ER environment is compromised, and the protein's folding capacity is impaired. The ER stress is able to activate an evolutionary conserved cascade since yeast to the mammalian a signaling events pathway known as UPR. The three "stress sensor proteins" have in common a similar structure, constituted of a ER luminal domain, an ER trans-membrane, and a cytosolic functional domain. All three ER stress receptors are maintained in an "inactive state" through their association with the ER chaperone, (GRP78/BiP) with their ER luminal domain. However BiP is more attracted by the misfolded protein added up inside the ER. This is the first signal of the ER encounter ER stress, BiP dissociates from the luminal domain of the three ER stress sensors, leading to activation of the UPR.

PERK is a transmembrane protein kinase of the PEK family, resident in the endoplasmic reticulum membrane. When it is free from BIP binding, the auto-phosphorylation of its kinase domain determines the ability to phosphorylate the alpha subunit of eukaryotic translation-initiation factor 2 (eIF2alpha).

The phosphorylated eIF2α is unable to recruit the methionyl tRNA to the 40S ribosoma subunit, thus causing a transient inhibitions of protein synthesis. (31)(32)

This event promotes cell survival by inhibiting the accumulation of nascent proteins arriving in the endoplasmic reticulum, thus restoring the ER homeostasis.
This experimental evidence was shown by the knockout of PERK (Perk - / -), that results sensitive to ER stress and resistant to the treatment with agents blocking the protein transcription such as Tunicamycin and Thapsigargin (33).
However, there are some proteins that are able to evade eIF2α-dependent translational block. Interesting Kaufman et al, 2016, suggested that the eiF2α phosforylation paradoxically enhances the presence of another transcription factor, ATF4, which promotes cell survival through the activation of genes involved in amino acid metabolism, redox reactions and protein secretion (34). Under prolonged or severe ER stress, ATF4 induces the transcription of C/EBP homologous protein (CHOP), considered a pro apoptotic factor, which is able to induce the expression of genes involved in the growth arrest and DNA damage 34 (GADD34). GADD34 activates phosphatase 1 that is able to restore the dephosphorylated status of eIF2a, therefore contributing to restore the protein synthesis system.
CHOP also induces ERO1a, which activates IP3R, favouring calcium release to mitochondria which results in cell death.
Moreover, PERK also contributes to nuclear factor-E2-related factor-2 (NRF2) activation and, consequently, to the expression of genes implicated in oxidative stress. In addition, PERK/eIF2a also induces cell cycle arrest by modulation of cyclin d1.(35)
Loss of function in PERK leads to apoptosis in situations of increased ER stress, resulting in permanent diabetes mellitus, multiple epiphyseal dysplasia, growth failure, and recurrent liver failure. Other findings have been described in association with Wolcott-Rallison syndrome (WRS), characterized by insulin-dependent diabetes in early infancy and, later, multiple system abnormalities.(34) Neuronal death in Alzheimer's and Parkinson's diseases is thought to be due to ER stress and has been weakly linked to PEK.(36)
I**RE1α** is a protein sensor that have a double enzymatic activity since is characterized by both a serin-treonin kinase domain and an endoribonuclease domain(37). In ER stress condition the detachment from BIP allow the dimerization and autophosphorylation that make active IRE1α, involved in the UPR response pathway.
IRE1α can determine a cleavages of 26 intronic nucleotides from XBP1 mRNA. The splicing variant generated XBP1s, encodes a stable and active transcription factor. (38) XBP1s moved inside the nucleus where will determine the transcription of genes coding for ER chaperons, for some ERAD components and for P58IPK, a member of the heat shock protein 40 (HSP40IPK) family p58IPK binds to PERK and began a negative feedback mechanism, removing the PERK-mediated translation block. P58IPK upregulation is not an immediate event, as its induction occurs several hours after PERK and eIF2α phosphorylation; it is therefore assumed that it can end the UPR when the ER's stress has now been solved (44). However, if the stress condition persists, P58IPK can induce increased transcription and synthesis of pro-apoptotic proteins (45).
Although the activation of IRE1 and the splicing of XBP1 mRNA seem to be events more implicated in cell survival, as they determine the induction of transcription and synthesis of chaperones proteins GRP78 and GRP94 and of P58IPK has been shown that IRE1 overexpression can also induce death by apoptosis in HEK293T cells (46).
This pro-apoptotic effect of IRE1 would seem to be mediated by the activation of the JNK kinase (47). In particular, the IRE sensor1 was seen to be able to recruit the TNF-receptor-associated factor 2 (TRAF2) adapter molecule; the TRAF2-IRE1 complex that is formed in turn, activates a pro-apoptotic signal through the induction of Apoptosis Signal Regulated Kinase (ASK1), a Mitogen Activated Protein Kinase Kinase Kinase (MAPKKK), which, at its time transmits the death signal to MAPKs JNK and p38 Once activated JNK is responsible for the phosphorylation of bcl2, thus suppressing its antiapoptotic activity(48) ;moreover, it is

able to determine the phosphorylation of the pro-apoptotic protein BH3 / BIM, in this case enhancing its pro-apoptotic effect (49) .

ATF6α. In mammals, there are two ATF6 isoforms, named ATF6α (90 kD) and ATF6β (110 kD).

ATF6α is a type II of transmembran protein of ER and its luminal domain is responsible for detecting misfolded proteins. The citoplasmatic domain instead contain the DNA domain useful to acts as transcriptional factor. After BIP dissociations, ATF6α moved into the Golgi apparatus, where is cleaved by a proteolytic cut in the juxtamembrane domain, by the serine proteases S1P and metallo proteases S2P, generating an active transcription factor p50ATF6α (50) . The p50ATF6α so, can entry into the nucleus and induces the transcription of genes that have an ER response element (ERSE) in their promoter (51). This target genes of ATF6α include : chaperons proteins, such as GRP78, GRP94, PDI, transcription factor GADD153/CHOP and for X box-binding protein1(XBP1).In particular ATF6α cooperates with the IRE1 sensor in the induction of XBP1 mRNA expression which, is subsequently subjected to endoribonuclease splicing by IRE1 the p50ATF6α activation is responsible for increasing the ER's ability to fold proteins, contributing to the restoration of initial homeostasis. Although ATF6 α can induce transcription of CHOP, a link between ATF6 induction and ER-induced apoptosis has not yet been demonstrated; indeed generally ATF6 mediates pro-survival signals in order to counteract the effect of ER stress (52).

ATF6α may have a role in the adaptation to chronic stress and it was evidenced in experiment that explored the responsiveness to stress in *Atf6*$\alpha^{-/-}$cells mouse, showing that in *Atf6*$\alpha^{-/-}$cells do not displayed basal stress than wild-type cells given an equivalent stimulus. Although the mechanism is not yet clear, ATF6α appears to suppress production of GADD34 during ER stress, allowing PERK/eIF2α signaling to persist and presumably contribute to maintenance of ER and general cellular function during chronic stress . ATF6α could to have the opposite effect of IRE1α signaling, as ATF6α deletion causes IRE1α to remain activated during chronic stress, although it is not yet clear whether this effect arises from(52). In general we may therefore conclude that in the presence of ER stress the activation of the IRE1 sensor would play a critical role in the initiation of pro-apoptotic signals, while the activation of the PERK and ATF6 sensors would seem to precede the activation of IRE1 in an attempt to resolve stress in the presence of a pro-survival action. If stress persists, the PERK and IRE1 pathways can converge, mediating the induction of the apoptotic process through mutual enhancement.

1.1.5 The UPR pathway in Chronic Disease and Cancer

Several studies reveled as metabolic conditions including hyperlipidemia, hyperhomocysteinemia, hyperglycemia, and inflammatory cytokines contribute to impair the protein folding in the ER. Kaufman et al, in 2002. Mutations affecting the ER stress–activated pancreatic ER kinase (PERK) and its downstream effectors, the translation initiation complex eukaryotic initiation factor 2 (eIF2), have a profound impact on cells development, function, and survival. PERK mutations are associated with the Wolcott-Rallison syndrome of infantile diabetes and mutations that prevent the α-subunit of eIF2 from being phosphorylated by PERK, block βcell development, and impair gluconeogenesis. UPR function is required by all cells to ensure that proteins in the secretory pathway are efficiently processed. (53) There is a strong, poorly understood link, between UPR activation and lipid accumulation in hepatocytes (steatosis), (54) as well as association with Fatty liver disease (FLD) ,actually considered like an emerging global epidemic.

The spread ability of tumors is made up of several events, that happen consequently or in parallel manner, such as hypoxia, glucose deprivation, lactic acidosis, oxidative stress, and inadequate amino acid supplies, that results to compromise protein folding in the ER. All three UPR mediators, such as PERK, ATF6, and IRE1α were found over-expressed in different types of cancer, including glioblastoma, multiple myeloma, and carcinomas of the breast, stomach, esophagus, and liver (55, 56).

In some works was reported the over-expression of the chaperone BIP/GRP78, that are induced by physiological stress conditions such as hypoxia, low pH, and glucose deprivation, that are very common conditions in the solid tumors microenvironments. The activation of stress pathway occurs in response to several pro-apoptotic stimuli and in vitro experiments demonstrated a correlation between induced expression of GRP78 and resistance to apoptotic death induced by topoisomerase II-directed drugs. This has been clearly demonstrated in breast cancer, in which the microenvironment have the capacity to induce the overexpression of specific genes encoding chaperone that acted in resistance to apoptosis and decreased chemotherapeutic efficacy. A similar situation was found also in hepatocellular carcinoma (HCC) progression. (57)

A study published on NATURE in 2009, investigating somatic mutations in several set of human cancer genomes to identify the relative contribution on carrying driver mutation under the gene-specific selection pressures, reported somatic mutations of the IRE1α gene (ERN1) in some human solid tumor. (58)

Numerous clinical studies have demonstrated that the hypoxia is a physiological ER stress condition common to all solid tumors, able to predict an increased malignant phenotype and metastatic potential of tumor cells. The link between hypoxia and cancer has long been eviscerated with the final aim of improving anti-cancer treatments. (59). demonstrated that translational control of protein synthesis during hypoxia occurs through the activation of PERK. These investigators showed that $PERK^{-/-}$mouse embryonic fibroblasts where unable to phosphorylate eIF2α and had decreased survival during hypoxia, when compared with wild-type mouse embryonic fibroblasts. They concluded that PERK plays an important role in hypoxia-induced translation attenuation, additionally supporting a role for hypoxia as an inducer of ER stress. (60)

Fujimoto et al., reported the overexpression of human XBP-1 gene in four cases out of five primary colorectal carcinomas and in four cases out of six colorectal adenomas. Also all four cancer cell lines expressed XBP-1 mRNA, confirming the data emerging from a previous work, showing the over expression of XBP-1 in all 11 primary breast and 5 breast cancer cell lines. In both these works authors concluded that XBP-1 expression could induce the impairment of cells differentiation regulation, playing an important role in carcinogenesis by accelerating tumor cells growth. (61, 62)

In addition XBP-1 was described as directly implicated in the hypoxic stress and tumor growth. Indeed hypoxia induced XBP1 at transcriptional level and activated splicing of its mRNA. After hypoxia exposure, apoptosis increased and clonogenic survival decreased in XBP1-deficient cells. Loss of XBP1 severely inhibited tumor growth due to a reduced capacity for these transplanted tumor cells to survive in an hypoxic microenvironment. (63)

A recent study reveals a post-transcriptional regulation of the early Ras phenotype, showing that oncogenic HRas induces ER stress and the activation of IRE1α. Indeed at the earliest stage of tumorigenesis, the oncogenic Ras triggers ER stress by activation of MEK-ERK pathway, causing up-regulation of IRE1 and splicing of XBP1 in primary epidermal keratinocytes. The reduction of ER stress and XBP1 splicing might induce keratinocytes into growth arrest and senescence, which can be further amplified by increased phosphorylation of ERK1/2. Consequently, phosphorylated ERK1/2 stimulates IRE1α hyper-activation and constitute a positive feedback loop under reduced ER stress. (64)

Further investigations demonstrated that XBP1u overexpression induced tumorigenesis by binding to, stabilizing, and activating mouse double minute homolog 2 (MDM2), an oncogene belonging to the RING domain-containing E3 ligase family and functions as a negatively effector of p53. XBP1u contributes also to the degradation process by ubiquitination of p53 and to the down-regulation of p21. (65)

As previously referred in the text , IRE1α mediates XBP-1 mRNA splicing, leading to the production of an active transcription factor XBP-1-p, which is involved in the regulation of VEGFA mRNA expression under ER stress conditions. Ghosh at al., showed that the IRE1α-XBP-1, PERK-ATF4, and ATF6α pathways can independently

regulate VEGFA mRNA expression under ER stress conditions useing different regulatory regions inside the VEGFA gene. (66)

UPR supports tumor cells growth and survival, both in the homeostatic and under ER stress conditions. PMID:25387057. Despite the overwhelming evidence of ongoing ER stress and UPR activation in many types of cancer, whether these processes ultimately inhibit or promote tumor growth in patients remains an area of intense investigation. (67)

The multiple myeloma (MM) evolves from a highly prevalent premalignant condition termed MGUS. In humans, the *XBP-1* gene has not been implicated in MM pathogenesis because it does not reside in a region targeted from chromosomal amplification and/or translocation in human MM tumors. However, there is evidence that the genes affecting *XBP-1* processing are subjected to genetic changes, potentially leading to epigenetic dysregulation of the XBP-1 network in MM. Using an engineered MM-prone model, a research group investigated the pathogenetic role XBP-1s expression in the neoplastic transformation of plasma cells. In mice, IRE1α and its homeostatic target XBP1 are both required for the differentiation of B lymphocytes into plasma cells. In addition, mice expressing a transgene of Xbp1s that did not have the 26-nt intron and hence required no further processing by IRE1α in B lymphocytes, developed a plasma cell malignancy closely resembling myeloma. (68)

The research approach over the last years has radically changed. Using a combination of whole-genome and whole-exome sequencing of primary tumors from 38 myeloma patients, researchers discovered XBP1 mutations in two of these patients. On further analysis, these mutations were shown to inactivate XBP1s, arguing against an obligate role for this transcription factor in myeloma. (69)

The FDA has approved molecule inhibitors of the ubiquitin proteasome pathway (UPP) called proteasome inhibitors for the treatment of multiple myeloma. Bortezomib (Velcade) is indicated as first-line therapy for myeloma patients, leading to myeloma cell death in part by preventing disposal of misfolded proteins through the ERAD pathway and thus triggering ER stress–induced apoptosis. On these basis, several pharmacologic inhibitors of the IRE1α RNase activity have been recently tested on human myeloma xenografts and were found to have antimyeloma activity. However, the specificity and off-target effects of these pharmacological agents are not well understood yet. (70, 71)

1.2 RATIONALE AND OBJECTIVES

Epidemiological studies have shown that chronic inflammation predisposes individuals to various types of cancer, including gastric, esophageal, colorectal, liver, pancreatic, bladder, and lung. (72) The pivotal role of the tumor microenvironment (TME) in the development and progression of cancer have led to a reasonable increase of efforts on studies focused to characterize the different components of such heterogeneous network and identify novel therapeutic targets.

Considering the epidemic proportions of cancer, obesity, hepatic steatosis, and the concurrent prevalence of several inflammatory conditions, there is an urgent need to better understand the cellular intrinsic molecular mechanism supporting these pathological conditions.

Numerous environmental, physiological, and pathological insults disturb ER homeostasis, referred to as ER stress, in which a collection of conserved intracellular signaling pathways, termed the unfolded protein response (UPR), are activated to maintain ER function and preserve cell survival. However, excessive and/or prolonged UPR activation leads to the promotion of cell self-destruction through apoptosis.

We have carefully analyzed the knowledge in this field of research, particularly focusing on the molecular pathway involving Nupr1, which represents a common molecular factor of all these different pathologies, even not well characterized yet, in the condition of ER stress.

NUPR1 was described as a transcriptional factor involved in the regulation of various cellular stress-response genes, including ER stress. Recently (73) it has been demonstrated that the transcriptomes of NUPR1 KO mice pancreata present a strong downregulation of mRNAs genes related to ER stress, suggesting that the presence of NUPR1 could play a crucial role in the physiological ER stress response.
Although several evidences demonstrated that NUPR1 is able to activate several downstream genes in the UPR pathway, however the specific biological mechanisms underlying NUPR1 activity under ER stress conditions remains still to be established. For this reason we tried to use known mouse models that determine a suitable study condition to explore the effect of Nupr1 in the ER stress in physiological conditions.
Hepatocytes, like other secretory cells, are rich in ER. Due to their high protein synthesizing capacity it is easy to postulate that UPR/ER stress response plays an important role either in preventing or mediating pathological changes in various liver diseases. Despite the identification of upregulation or dysregulation of ER stress signaling mediators in various forms of liver injury, and the rapid expansion of research in the field of ER stress in liver diseases, the exact contribution of ER stress response to many forms of hepatic injury remain to be fully established.

In the present work we aim to explore how NUPR1 interacts with some pivotal genes that are the major modulators of the ER stress and metabolic cell function. In particular we investigated the biochemical and molecular effects arising from the loss of NUPR1 in ER stress physiological conditions.

CHAPTER 2

Materials and Methods 2

2.1 ANIMAL MODELS.

For the study of chronic ER stress in physiological conditions, we used *Nupr1*$^{-/-}$ mice bearing a homozygous deletion of P8 exon 2 (74) to be bread at the experimental conditions and *Nupr1*$^{+/+}$ mice as genotype control, both wild type for Cre and KRas genes.

They were kept in the Experimental Animal House of the Centre de Cancérologie de Marseille (CRCM) of Luminy. All experimental procedures carried out on animals were approved by the Comité d'éthique de Marseille numéro 14a in accordance with the European Union regulations for animal experiments.

All the animals were housed in a room maintained at a controlled temperature of 24 ± 2 °C under a 12-h light-dark cycle. Animals were allowed ad libitum access to standard pellet chow and water since the beginning of the project. All experiments were carried out in accordance with the Animal Experimentation Guidelines of European Union.

2.2 ACUTE ER STRESS

To induce ER stress in liver cells, we injected a single intraperitoneal dose of 1 μg/g body weight of tunicamycin in 150 m*M* dextrose. The mice were euthanized, and the livers dissected for the following experiments: (1) approximately 50 mg fresh liver tissue was homogenized for the purification of liver total RNA using Trizol reagent (Invitrogen); (2) approximately 100 mg fresh liver tissue was homogenized for preparation of liver protein samples for Western blot assay and a small piece of fresh liver tissue (about 50 mg) washed briefly with phosphate-buffered saline (PBS) and then fixed in 4%PBS-buffered formalin. Fixed liver samples were paraffin embedded, and 4-μm sections have been prepared and mounted on glass slides for immunohistochemical staining. The remaining liver tissue was snap frozen in liquid nitrogen and stored at 80 °C for future use.

2.3 CHRONIC ER STRESS

Two groups of mice were respectively fed with a high-fat diet (HFD) (catalog number: D12451, 45 kcal% fat, Research Diets) for 15 weeks to generate a ER stress physiological conditions, and to a normal diet (ND) (catalog number: D12450H, 10 kcal% fat, Research Diets, New Brunswick, NJ, USA) for 15 weeks as control group. Female mice are protected against HFD-induced metabolic changes while maintaining an anti-inflammatory environment in the intra-abdominal adipose tissue with an expanded T(reg) cell population, whereas HFD-fed male mice develop adipose tissue inflammation, glucose intolerance, hyperinsulinemia, and islet hypertrophy. (75) Therefore for our experiments we used exclusively male mice.

There was no significant difference in initial body weight among the two groups (mean body weight of ND group = 18.36 ± 0.41 g, mean body weight of HFD group = 18.70 ± 0.40 g, p = 0.61). Body weight gain and feed consumption were monitored weekly to determine the feed efficiency ratio (FER).After the end point of experiment, the mice were sacrificed. The blood samples were collected by cardiac puncture, centrifuged at 800 g for 10 min at 4 °C, and the serum was stored at −80 °C. The livers were collected, weighted, and stored at −80 °C.

The mice were sacrificed by asphyxia procedure in CO2. The livers s removed, flash frozen in liquid nitrogen and stored at -80°C for RNA and protein analysis

2.4 GENOTYPING

P8 genotyping procedures by PCR-end point were performed on DNA genomics isolated from fragments of tails in according to the manufacturer's protocol.
(See ***SUPPLEMENTARIES TABLE A and TABLES 5.1.1/5.2***)
The mutationals status of P8, Cre and KRas genes was assessed by Terra PCR Direct Red Dye Premix (Clontech, 639286) using a 96 micro wells thermo cycler. (See ***SUPPLEMENTARIES TABLES 5.2)5.2.1-5.2.4)***

2.5 WESTERN BLOT

The Western blot is one of the most common techniques used in molecular biology to detect the presence of protein targets in complex samples.

2.5.1 Sample collection and preparation.

Protein lysates are a mixture of debris, fats, hydrophobic protein aggregates, nucleic acids, and proteases and it is important to use cell lysis buffers and homogenization techniques that eliminate their effects from western blots.

2.5.2 Protein production and purification.

Protein extraction (76) was performed since free tissue of mice sacrificed and placed in crio-tube immersed in liquid nitrogen and conserved at minus 80°. The homogenization was obtained in a radio immunoprecipitation assay buffer (RIPA), with a protease inhibitor cocktail (Sigma) and 5µL NaF 1mM, 50 µL Na_3VO_4 100 µM, 200µL βGlycerol-P, 50µL PMSF 1% 1mM, 4.670 mL of RIPA (Na deoxycholate 10% (1M) SDS 20% 0.1M , TRITON-X 100 1% ,TRIS BASE pH8 2M , NaCl 5M). ***SUPPLEMENTARIES BUFFER 5.1.3-5.1.4*)**
The optimal condition to process the samples are performed using (for the homogenization) the Precellys® developed by Bertin Technologies that lysed and homogenized the biological samples by a specific movement, called precession. The protocoll expects 3 cycle for 15 sec at 6500 RPM .Proteins were purified by centrifugation at 14,000 × *g* at 4 °C for 20 min and subsequently quantified by BCA Protein Assay (Pierce™ BCA Protein Assay Kit thermo Fischer cata.#23225)and read by the The FLUOstar® Omega. Upon determined the protein concentration we took for the loading 40 µg and add the Laemmli for the denaturations for 5 minutes inside the thermo mixer at 95°.

2.5.3 Separation, Transferring and Data analysis

For western blot analysis, 25 µl of protein were separated by electrophoresis into a 7%/10% /12%polyacrylamide protein gel (SDS–PAGE) (10 cm x 10 cm)under denaturing (SDS) and reducing (β-mercaptoethanol) conditions for 1.5 h at 80-110 V ; the transferred to a nitrocellulose membranes ULTRA CRUZ NITRO (0.22µm) were performed at 225 mA at maximum voltage during 2 h. (***SUPPLEMENTARIES BUFFER 5.1.2*)**
Then, the nitrocellulose membranes were blocked 1 h with a solution of 5% (w/v) BSA in TBS Tween 0,1%, or 5% of dry milk TBS Tween 0,1% and incubated overnight, at 4 °C, with a primary antibody;(***SUPPLEMENTARIES BUFFER 5.1.2***)
The antibody used were ATF4 (D4B8) rabbit mAb (1:1000 Cell Signaling #11815) 49 kDa, AT Vasseur et al. 2002 F6(D4Z8V) rabbit mAb (1:1000Cell Signaling #65880) 90-100 kDa, BIP (C50B12) rabbit mAb (1:1000,Cell Signaling #3177)78 kDa, XBP1s antibody(1:1000Cell Signaling #83418) mouse 55kDa, Chop (L63F7) mouse mAb (1:1000Cell Signaling #2895), Phospho-PERK (Thr980) (16F8) Rabbit mAb(1:500Cell Signaling #3179 **)** 170 kDa;
After that the nitrocellulose membrane was washed with TBS Tween 0.1% three times for 5 minutes and at this point we incubated the membrane with the secondary antibodies, using 1:1000 -1:3000 dilution in blocking solution for 1 h at room temperature.

The last procedure consist in re wash the membrane-bound HRP (antibody conjugate) for 3 times in TBST, and once exposed in Peroxidase activity was detected by enhanced chemiluminescence kit (PerkinElmer Inc, Waltham, MA, USA) detected in a G-Box (Syngene).(***SUPPLEMENTARIES TABLES 5.3.1***)

2.6 TRANSCRIPTIONAL PROFILE ANALYSIS

2.6.1 Genes Classification

We tested Gene expression profiles for the major gene involved in the following cellular pathways:

ER stress response:

ATF4 - activating transcription factor 4
ATF6-- activating transcription factor 6
CHOP -CCAAT/enhancer-binding protein (C/EBP)
GADD34- Growth Arrest and DNA Damage-inducible protein
XBP1u - X-box binding protein 1u
XBP1s -X-box binding protein 1s
HyOu -hypoxia up-regulated 1
ERDJ4 -DNAJB9 DnaJ heat shock protein family (Hsp40) member B9
HYOU Hypoxia Up-Regulated 1
GRP94 HSP90-Like Protein chaperone
BIP/ GRP78 chaperone or Immunoglobulin heavy chain binding protein

Metabolism Sindrome genes:

Lipogenesis:

SREBP1C central lipogenic regulator-sterol regulatory element binding protein
ACLY - ATP citrate lyase
LCB3- Long-chain base-1-phosphate phosphatase
ChREBP or MLXIPL MLX interacting protein like

Lipoprotein:

APOB -apolipoprotein B
PPARα -peroxisome proliferator activated receptor alpha
MTTP- microsomal triglyceride transfer protein

GLYCOLYSIS METABOLIMS

PGK1 phosphoglycerate kinase 1

Fatty Acids Metabolism

LCAD- Long chain acly-CoA dehydrogenase
MCAD -Medium chain acyl-CoA dehydrogenase deficiency
FAS/FANS Fatty Acids Syntetase
SCD1 -Stearoyl-CoA desaturase
FABP1 Fatty acids binding proteins

BETA OXIDATION

Acox1 Fatty acyl-coenzyme A oxidase
CPT-1A-carnitine palmitoyltransferase-1a
CPT-1b -carnitine palmitoyltransferase-1b

Triglyceride synthesis

DGAT1 acyl-CoA:diacylglycerol acyltransferase-1
DGAT2 acyl-CoA:diacylglycerol acyltransferase-2

Membrane transporter

SLC27α- (Solute Carrier Family 27 Member 1)
MCT4 Monocarboxylate transporters (MCTs)

Transcriptomic profiles were determined from mRNA samples collected from: Nupr1 $^{-/-}$ and Nupr1 $^{+/+}$ HFD mouse model and the same genotypes maintained in normal chow diet.

2.6.2 RNA Extraction.

RNA was isolated from fresh tissues using TRIzol (Invitrogen CAT.NUM.15596018), according to the manufacturer's protocol In brief, approximately 100 mg organs were homogenized in 1mL of Trizol reagent..(***SUPPLEMENTS TABLE 5.4.1-5.4.2***) . RNA concentration was determined by the absorbance at 260 nm Microplate Spectrophotometer (Epoch BioTek) and the RNA quality and integrity (RIN value) was verified by Agilent Technology 2100 bioanalyzer in RNA 6000 Nano chip Kit. (***SUPPLEMENTS TABLE 5.4.3-5.4.4)***

2.6.3 Reverse Transcriptase. Polymerase Chain Reaction Analysis

cDNA was synthesized using 1 µg of total RNA and GoScript Reverse Trascriptase. (PROMEGA CAT#.A5001). GoScript™ Reverse Transcriptase cDNA synthesis is designed to convert up to 5µg of total RNA or up to 500ng of poly(A) RNA into first-strand cDNA. In the first steps experimental RNA is combined with the experimental primer. The primer/template mix is thermally denatured at 70°C for 5 minutes and chilled on ice. A reverse transcription reaction mix is assembled on ice to contain nuclease-free water, reaction buffer, reverse transcriptase, magnesium chloride, dNTPs (PCR Nucleotide Mix) and ribonuclease inhibitor.

Samples were then incubated at 25 °C for 5 min ,42 °C up to 60 min and70° for 15 minuti, cooled to 4 °C for 5 min. (***SUPPLEMENTS TABLE 5.4.5-5.4.6-5.4.7)***

2.6.4 Real-Time Polymerase Chain Reaction Analysis

The GoTaq qPCRMaster Mix (PROMEGA CAT.#A600A) (containing the fluorescence enhancement SYBR® Green), CXR Reference Dye (PROMEGA CAT.#C541A) free water and gene-specific primers were amplified using a AriaMx Real-time PCR System (Agilent), There are various studies regarding the identification of suitable house keepings genes (HKGs) for RT-PCR. We chose to normalize, the selected reference genes levels by the housekeeping gene RPLP0 *(5'GGACCCGAGAAGACCTCCTT3';* 5'*GCACATCACTCAGAATTTCAATGG,3')* (Applied Biosystems). The RT-qPCR program was comprised of predenaturation at 95°C for 1 minute, 40 cycles at 95°C for 20 seconds, 60°C for 15 seconds, and 72°C for 15 seconds. ***(SUPPLEMENTS TABLE 5.5)***

Relative genes expressions quantifications was performed using the simple ΔCt approach was employed by comparing relative expression of 'pairs of genes' within each sample by AriaMx - Analyzing a Comparative Quantitation Experiment software.

2.7 LIVER INFLAMMATION AND STEATOSIS

2.7.1 Oil Red O Staining

Using Oil Red O Stain Kit (Lipid Stain), (ab150678) we performed a histological visualization of fat cells and neutral fat on frozen tissue **.** After realized the fresh or frozen tissue sections we proceed with a succession of incubations according the manufacturer's protocol of Oil Red O staining protocol. Lipid droplets in mature adipocytes then stained with Oil Red O staining solution was observed by Nikon Eclipse 90i microscope.

2.7.2 Alanine Aminotransferase activity

We indirectly tested liver inflammation and steatosis status using Alanine Aminotrasferase (ALT) assay KIT (Sigma-Aldrich catalog number MAK052.

According with the manufacturer's protocol the ALT activity measured the ALT activity in the serum samples of Nurp-/- and Nurp+/+mouse in HFD and normal chow diet. in accordance with the manufacturer's instructions. In addition we assessed ALT activity in the same genotypes models after Tunicamicyn induced acute ER stress.

ALT, known as serum glutamic-pyruvic transaminase (GSPT) belong to the pyridoxal-phosphate- dependent enzymes, and is able to catalyze reversible transfer of amino group from alanine to α-ketoglutarate, generating pyruvate and glutamate.

ALT activity is determined by a coupled enzyme assay which result in a colorimetric (570 nm)\fluorimetric (587nm) product, proportional to the pyruvate generated. Both the colorimetric and fluorimetric assay require 1 to 20 µl of sample for each reaction. Serum sample can be directly added to wells (1-20 µl). Samples must be brought to a final volume of 20 µl with the ALT Assay Buffer (catalog Number MAK052A). For the

positive control may be added 5 µl of ALT positive control (catalog Number MAK052F) to wells. The final well volume must be adjusted to 20 µl with ALT Assay Buffer (catalog Number MAK052A) .
After dispensed the Master Mix reaction according to the kit instructions the well need to be incubated with measurements taken every 5 minutes. The FLUO start Omega has been used for the well reading.
The ALT activity of a sample may be determined by the following equation: (reported as nmole/min/mL)
ALT Activity

B = amount (nmole) of Pyruvate generated between T inizial and T final
T inizial = time of first reading in minutes
T final = time of penultimate reading in minutes
V = sample volume (mL) added to well.

2.8 STATISTICAL ANALYSIS

In this study we used the ΔCt method , defined as the number of cycles needed for the fluorescence to reach a specific threshold level of detection and is inversely correlated with the amount of template nucleic acid present in the reaction. Here we employed a ΔCt method by comparing relative expression of 'pairs of genes' and in each pairs one is the useful housekeeping genes. .In order to obtain the most real value we properly evaluate, a minimum of 3 replicates . Downregulated gene has a scale of 0-1, while upregulated gene has scale of 1-infinity
Statistical analysis was performed using GraphPad Prism version 6 (GraphPad, La Jolla, CA, USA). All results are expressed as mean ± SEM unless otherwise indicated.
For the qRT-PCR experiments, the Holm-Sidak method was used to perform multiple t tests at once. Error bars indicate standard deviation of the means. * $p<0.05$, ** $p<0.01$, and ***$p<0.001$ relative to vehicle control by multiple t test with correction for multiple comparisons. For the Western Differences were considered significant at a p value <0.05 and the values presented in the figures are $p<0.05$, **$p<0.01$, and ***$p<0.001$.

CHAPTER 3

Results 3

3.1 NUPR1-DEFICIENCY LEADS TO A LACK OF ACTIVATION OF "ACUTE ER STRESS" RESPONSE PATHWAY *IN VIVO*

We reported the biochemical and molecular data obtained to investigate whether the lack of NUPR1 leads to alterations in in-vivo "acute ER stress" response. We performed Tunicamycin (Tun, 1.0 μg/g) injections in both NUPR1 wild-type (NUPR1+/+) and NUPR1 knockout (NUPR1-/-) mice. We have focused on the expression of the major UPR associated proteins 16h post-injection in liver extracts by Western Blot analysis. As shown in Figure 3.1.1 the expression of phospho-Ire1-α and the spliced XBP1s proteins occurred similarly in both $NUPR1^{+/+}$ and $NUPR1^{-/-}$ treated liver after Tun injections, suggesting that an effective activation of the Ire1-α branch of the UPR occurred. As expected, the increment of XBP1s mRNA in $NUPR1^{-/-}$ mice after stress induction was lower compared to $NUPR1^{+/+}$ mice. The two-way ANOVA analysis attested a significant effect (effect of Tun: $p<0.0001$; effect of genotype (NUPR1+/+vs NUPR1-/-)$p<0.0002$; interaction $p=0.0002$; NUPR1+/+ vs NUPR1-/- in Tun condition: $p<0.0001$ post hocSidak test, n=6). Interesting the chaperone BiP expression level was lower in NUPR1-/- mice compared to NUPR1+/+ mice (n =6). The two-way ANOVA analysis revealed a significant effect of Tun ;$p <0.0032$, a significant effect of the genotype (NUPR1+/+vs NUPR1-/-, $p< 0.0001$) and an interaction between the two factors ($p=0.0002$ for protein). Subsequent corrected multiple comparisons uncovered a significant difference between NUPR1+/+ and NUPR1-/- mice after Tun administration ($p<0.0001$ post hocSidak test), but not in control conditions. BIP is a stress sensor of the UPR and an integral part of the ER quality control system. Upon UPR initiation, the translational efficiency of BiP is normally increased by two to three folds and regulated by several overlapping mechanisms. (78)

As regards ATF6, we found a significant increase of ATF6 protein expression in $NUPR1^{-/-}$ mice after stress induction compared to $NUPR1^{+/+}$ mice. (effect of Tun: $p<0.0001$; effect of genotype $p<0.0001$; interaction $p<0.0001$; $NUPR1^{+/+}$ vs $NUPR1^{-/-}$ in Tun condition: $p<0.0001$, post hocSidak test, n=6). Our data are similar to those reported in another work, published in 2011, sustaining that tunicamycin treatment induces ATF6. (79).

Both the expression of eif2alfa and the Phosphorylation of PERK occurred without significant variation between the two genotypes. However, the protein expression of ATF4, which is directly correlated with p-PERK activity, was significantly downregulated in $NUPR1^{-/-}$mice after ER stress induction compared to $NUPR1^{+/+}$ mice. Thus, we hypothesized that NUPR1 could act downstream of the PERK branch within the UPR complex. This hypothesis was supported by absence of the CHOP protein expression in NUPR1-/- mice (effect of Tun: $p < 0.0001$; effect of genotype $p < 0.0001$; interaction $p < 0.0001$;$NUPR1^{+/+}$ vs $NUPR1^{-/-}$ in Tun condition: $p < 0.0001$, post hocSidak test, n=6). These data confirmed that the absence of NUPR1 led to an inefficient activation of the PERK branch of the ER stress response.

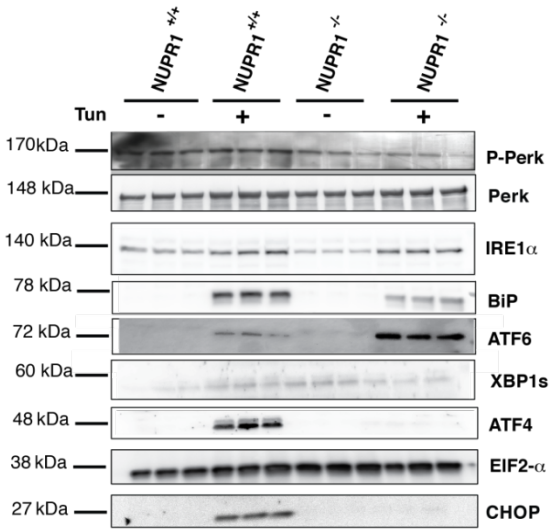

Fig 3.1.1 General decrease in ER associated protein expression in NUPR1$^{-/-}$ mice after stress and at basal level in hepatocytes injected with Tunicamycin (Tun, 1.0 µg/g).

In figure 3.1.2 are reported the sections from NUPR1$^{+/+}$ (A and C) and NUPR1$^{-/-}$ (B and D) mice at baseline and post 16 h Tunicamycin (1.0 µg/g) injection (C and D).
A) The ER is organized into a netlike labyrinth of branching tubules and flattened sacs extending throughout the cytosol. The hepatocyte cells are the principal site of production of lipoproteins, enzymes that catalyze a detoxify reactions required by ER membrane C) After the treatment and under effect of Tun the ER lacks the regular organizations as result of the increasing of misfolded protein and of the ER stress condition. Moreover we can see how the mitochondria are present inside the ER structure. B) for NURP1$^{-/-}$ the ER is less organized respect the wild type liver cells. D) after the Tun injection the mitochondria broke the ER lamellar structures and the MAMs associations become visible. MAMs play a critical role in the transmission of physiological and pathological signals from ER to mitochondria. Moreover, recent studies have shown that the induction of a persistent ER stress could represent a checkpoint in the regulation of the initiation phase of the mitochondria-mediated apoptotic pathway (80). Therefore, ER could be considered as the site where apoptotic signals are generated and integrated in order to induce cell death.

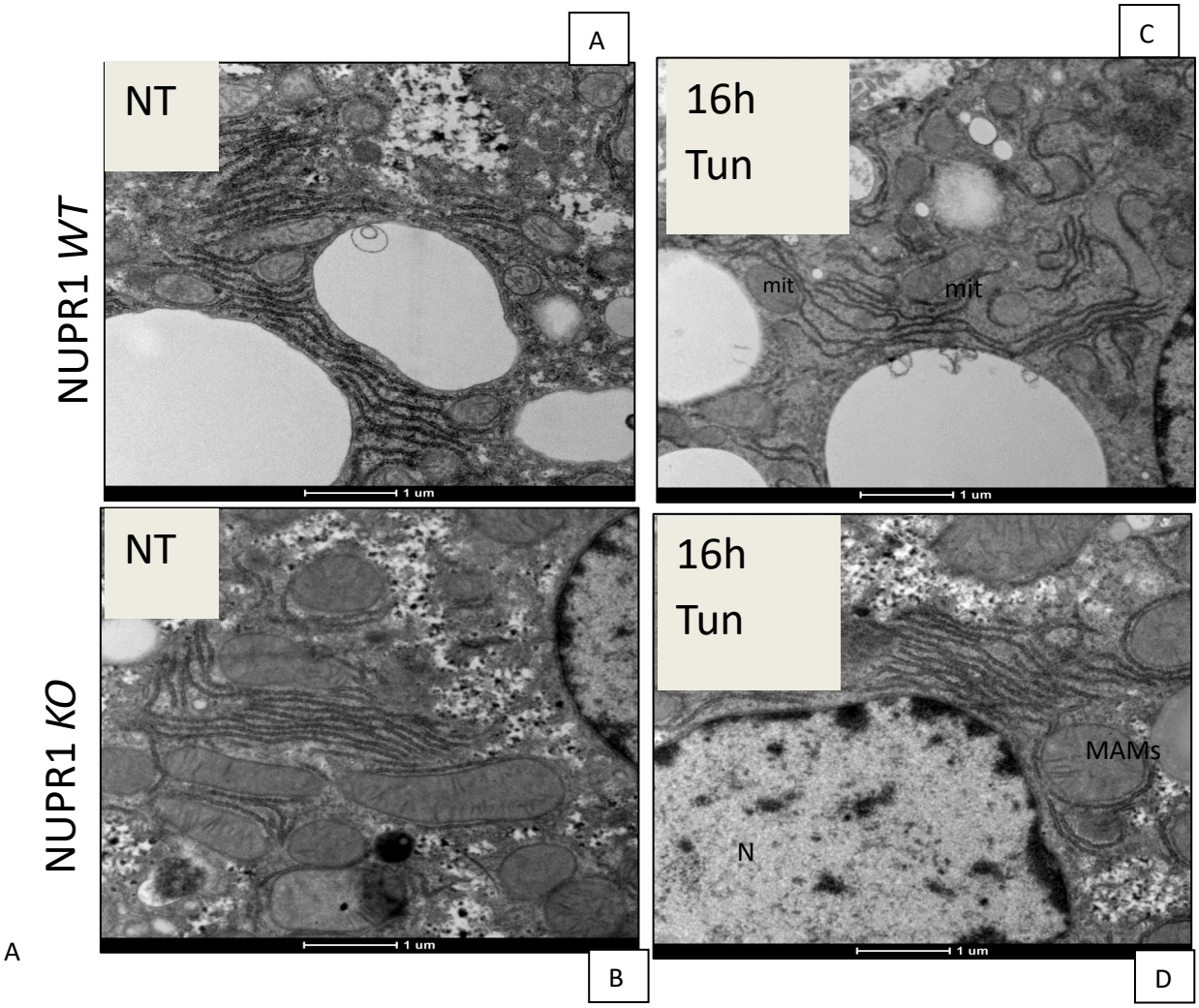

Fig. 3.1.2 Micrograph of NUPR1 wild type$^{(+/+)}$ and NUPR1 knockout $^{(-/-)}$murine hepatocytes after 16h Tunicamycin injection (1.0 µg/g) .

Insets for each image higher magnification sections. Black arrows point to ribosomes on the ER cisternae. Asterisks point dilated ER cisternae. Abbreviation used N=nucleus; zy=zymogen granules; mit=mitochondria

3.2 NUPR1-DEFICIENCY LEADS TO A LACK OF ACTIVATION OF "CHRONIC ER STRESS" RESPONSE PATHWAY *IN VIVO AFTER HFD 10 WEEKS.*

To generate chronic ER stress physiological conditions, we imposed a high fat diet (HFD) feed for 10 weeks to the male mice, whose body weight gain and feed consumption were monitored weekly to determine the feed efficiency ratio (FER). There was no significant difference in initial body weight among the two groups (mean body weight of ND group = 18.36 ± 0.41 g, mean body weight of HFD group = 18.70 ± 0.40 g, p = 0.61). Feeding NUPR1 $^{+/+}$ and NUPR1 $^{-/-}$ male mice ad libitum a solid, fat based, high-fat diet (HFD) resulted in a continuous and modest bodyweight gain within a period of 10 weeks (Fig.3.2.1). The body volume of NUPR1 $^{-/-}$ mice increased significantly at 4,5,6 weeks by multiple t test (p= 0,000043, p= 0,000243, p= 0,00483). The liver weights and intra-abdominal fat increased in NUPR1-/- HFD mice in accordance to the total body weights.

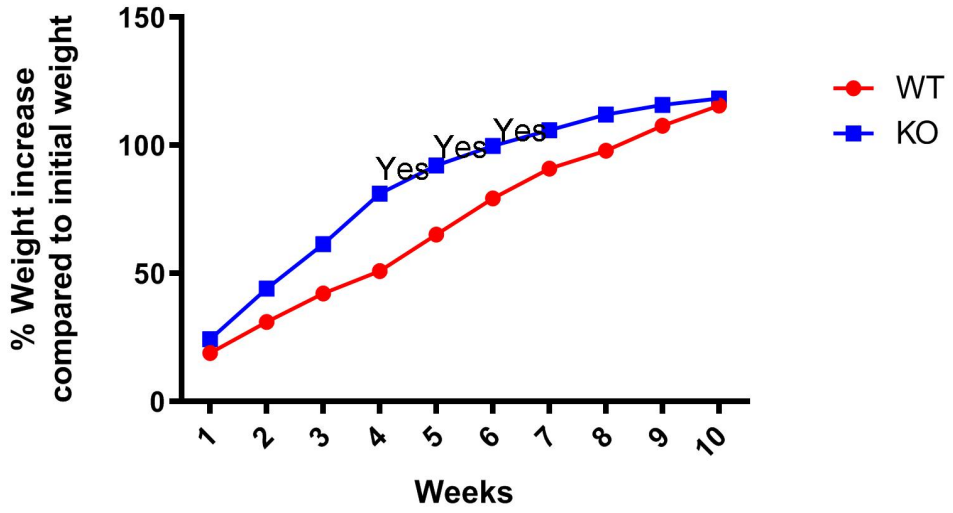

Figure 3.2.1 Body weight monitoring during 10 weeks of HFD regime in NUPR1 knockout $^{(-/-)}$ (blue) and NUPR1 wild type$^{(+/+)}$ (red) mice

We compared *NUPR1* wild-type (*NUPR1*$^{+/+}$) and NUPR1 knockout (*NUPR1*$^{-/-}$) mice after 10 weeks of HFD condition with their respective *NUPR1* wild-type (*NUPR1*$^{+/+}$) and NUPR1 knockout (*NUPR1*$^{-/-}$) normal chow diet (ND) mice controls. Western blot and Real time-qPCR analysis were performed to evaluate the expression levels of the major UPR associated proteins at the first time point of 10 weeks HFD.

The collected data showed that the liver expression of the chaperone BIP protein was lower in *NUPR1*$^{-/-}$ HFD mice compared to *NUPR1*$^{+/+}$ HFD mice (n=5). Consistently, the BIP mRNA expression was downregulated in *NUPR1*$^{-/-}$*HFD* mice compared to *NUPR1*$^{+/+}$ HFD mice (n=5). For both protein and mRNA, two-way ANOVA analysis revealed a significant effect of diet (p=0.0003 for mRNA; p<0.0042 for protein), a significant effect of genotype (*NUPR1*$^{+/+}$ vs *NUPR1*$^{-/-}$, p=0.0002 and p< 0.0002) and a significant interaction between the two factors (p<0.0001 for mRNA; p=0.0002 for protein) (Figure 3.2.2 and 3.2.3). Subsequent corrected multiple comparisons uncovered a significant difference between *NUPR1*$^{+/+}$ and *NUPR1*$^{-/-}$ *HFD* mice (p<0.0001 for protein and mRNA analysis, *post hoc*Sidak test), but not in control conditions.

Both the expression of eIF2alfa and the Phosphorylation of PERK occurred without significant variation between the two genotypes (Figure 3.2.2). However, the mRNA expression levels of ATF4, which directly correlated with p-PERK activity, were significantly downregulated in *NUPR1*$^{-/-}$ HFD mice compared to *NUPR1*$^{+/+}$ HFD mice (effect of diet: p<0.0001; effect of genotype p<0.0001; interaction p=0,0200 *NUPR1*$^{+/+}$ vs *NUPR1*$^{-/-}$ in HFD: p=0.0004, *post hoc*Sidak test, n=5) (Figure 3.2.2 and 3.2.3). Accordingly, we observed lower levels for both CHOP protein and mRNA, in NUPR1$^{-/-}$ HFD mice compared to *NUPR1*$^{+/+}$ HFD mice (effect of diet: p<0.0001; effect of genotype p<0.0001 ; interaction p<0,0001 *NUPR1*$^{+/+}$ vs *NUPR1*$^{-/-}$ in HFD: p<0.0001 , *post hoc*Sidak test, n=5) (Figure 3.2.2 and 3.2.3).

As expected, both XBP1s protein and mRNA were less expressed in *NUPR1*$^{-/-}$ HFD compared to *NUPR1*$^{+/+}$ mice (effect of diet : p=0,0006; effect of genotype p<0.001 ; interaction p=0.0002; *NUPR1*$^{+/+}$ vs *NUPR1*$^{-/-}$ in HFD: p<0.0001 for protein and mRNA analysis, *post hoc*Sidak test, n=5) (Figure 3.2.2 and 3.2.3).

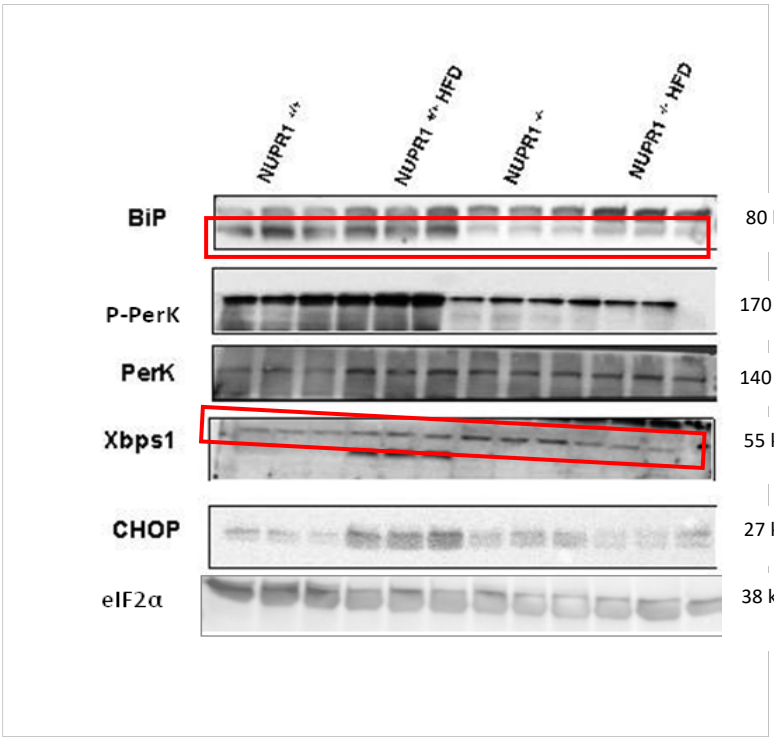

Figure 3.2.2 UPR associated proteins Western blots in NUPR1$^{-/-}$ and NUPR1 $^{+/+}$ 10 weeks HFD and ND control mice

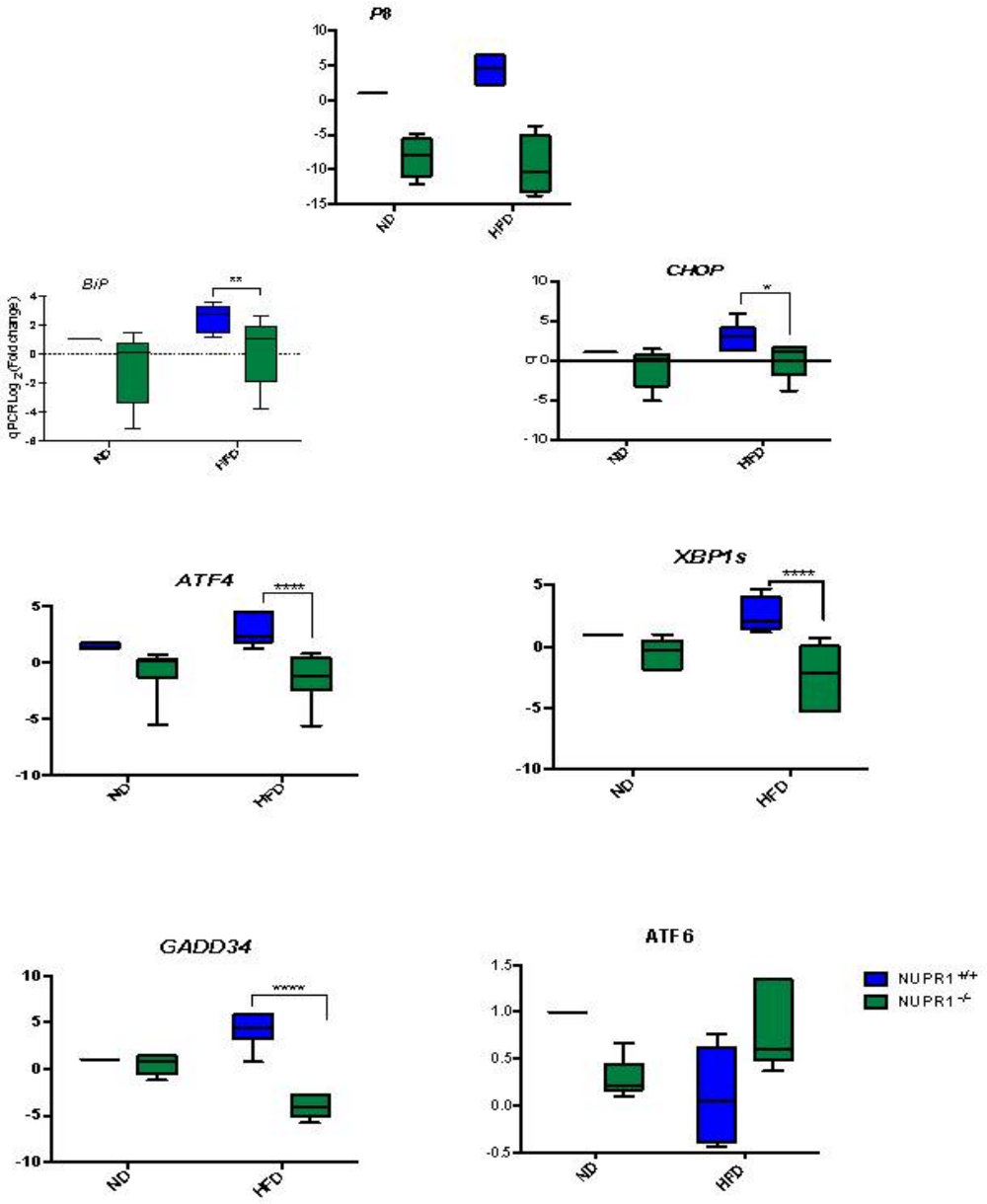

Figure 3.2.3. UPR associated genes RT-qPCR in NUPR1$^{-/-}$ and NUPR1 $^{+/+}$ 10 weeks HFD and ND control mice.

As observed in "acute ER stress" condition, we showed that in in-vivo models subjected to physiological ER stress after 10 weeks HFD, NUPR1 might act downstream of the PERK branch within the UPR complex. This hypothesis was supported by by the downregulation of BIP, ATF4 and CHOP in in-vivo *NUPR1*$^{-/-}$ HFD mice. A further confirmation to our hypothesis was provided by the downregulation of GADD34 mRNA expression level in *NUPR1*$^{-/-}$ HFD mice compared to *NUPR1*$^{+/+}$ HFD mice (effect of diet : p=0,0296*; effect of genotype *p*<0.0002*; interaction p=0.0002*; *NUPR1*$^{+/+}$ vs *NUPR1*$^{-/-}$ in HFD: P=0.0296* *post hoc*Sidak test, n=5). GADD34 is transcriptionally induced by stress gene, downstream of ATF4 and CHOP, and its translation escapes the general attenuation of protein synthesis resulting from eIF2α phosphorylation. (81)

3.3 NUPR1-DEFICIENCY LEADS TO A LACK OF ACTIVATION OF "CHRONIC ER STRESS" RESPONSE PATHWAY *IN VIVO AFTER HFD 15 WEEKS.*

In order to verify whether the effect of Nupr1 lack was maintained over the time, a second groups of mice were breaded at HFD condition for 15 weeks, with body weight gain and feed consumption weekly monitored to determine the feed efficiency ratio (FER). There was no significant difference in initial body weight among the two groups (mean body weight of ND group = 18.36 ± 0.41 g, mean body weight of HFD group = 18.70 ± 0.40 g, p=0.61).

As previously observed, feeding NUPR1 $^{+/+}$ and NUPR1 $^{-/-}$ male mice ad libitum a solid, fat based, high-fat diet (HFD) resulted in a continuous and modest bodyweight gain within a period of 15 weeks (Fig 3.3.1). The NUPR1$^{-/-}$ mice gained more weight than the matched NUPR1$^{+/+}$ group between the 6th and the 15th weeks; however such difference did not reach statistical significance in any of the evaluated timepoints (p:0,6588 at 15th week). Also in this case the liver weights and intra-abdominal fat were increased in NUPR1 $^{-/-}$ HFD mice in accordance to the total body weights.

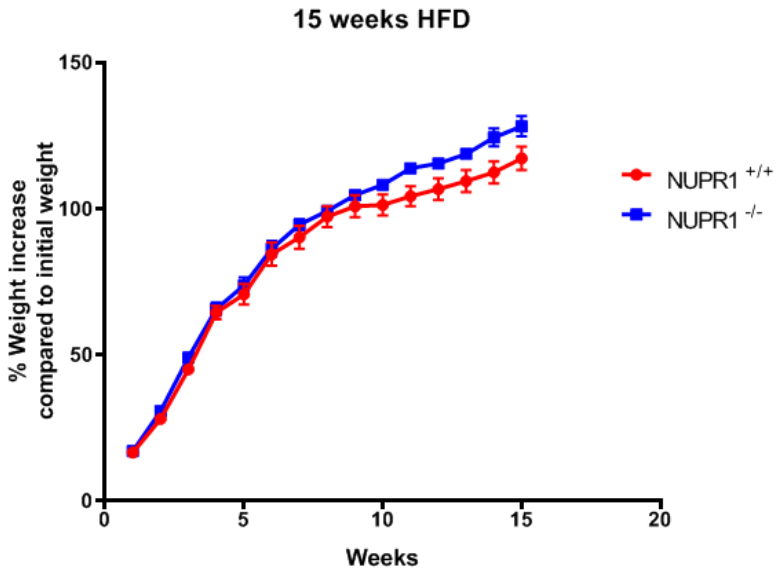

Figure 3.3.1 Body weight monitoring during 15 weeks of HFD regime in Nupr1$^{-/-}$ (blue) and Nupr1$^{+/+}$ (red) mice

To study whether the effect of NUPR1 protein lack is stored over time and to understand the molecular mechanisms underlying alterations in the pathophysiologic status of ER stress, we examined hepatic genes differentially expressed in a long-term (15 weeks) HFD, in *NUPR1* wild-type (*NUPR1*$^{+/+}$) mice and NUPR1 knockout (*NUPR1*$^{-/-}$) compared with their respectively normal chow diet (ND) controls.

Western blot analysis were performed to evaluate the expression levels of the following major UPR proteins: ATF6, XBP1s, CHOP, BIP and eIF2α.

As shown in Figure 3.3.2, a significant increase of ATF6 protein expression was observed in *NUPR1*$^{-/-}$ mice HFD, compared to *NUPR1*$^{+/+}$ mice (effect of diet: $p<0.0001$; effect of genotype: $p< 0.0001$); interaction $p<0.0001$; subsequent multiple comparison *NUPR1*$^{+/+}$ vs *NUPR1*$^{-/-}$ *15 weeks HFD* condition: $p<0.0001$, *post hoc*Sidak test, n=5). No significant differences were reported for eIF2α expression protein levels after 15 weeks of Chronic ER stress. The expression of XBP1s protein was significantly lower in *NUPR1*$^{-/-}$ mice HFD, compared to *NUPR1*$^{+/+}$ mice, (effect of diet: $p<0.0001$; effect of genotype $p<0.0002$; interaction $p = 0.0002$; *NUPR1*$^{+/+}$ vs *NUPR1*$^{-/-}$ *15 weeks HFD*: $p<0.0001$ *post hoc*Sidak test, n=5) (Figure 3.3.2).

The liver expression of the chaperone BiP in *NUPR1*$^{-/-}$ mice HFD is confirmed to be less expressed compared to *NUPR1*$^{+/+}$ mice HFD (n=5); the two-way ANOVA analysis revealed a significant effect of diet; $p <0.0032$, and genotype ($p<0.0001$), with an interaction between the two factors ($p=0.0002$). Subsequent corrected multiple comparisons uncovered a significant difference between *NUPR1*$^{+/+}$ and *NUPR1*$^{-/-}$ mice HFD ($p<0.0001$ *post hoc*Sidak test, n=5). The expression of CHOP in *NUPR1*$^{-/-}$ mice remained lower also after 15 weeks of HFD (effect of diet: $p<0.0001$; effect of genotype: $p<0.0001$; interaction $p<0.0001$; *NUPR1*$^{+/+}$ vs *NUPR1*$^{-/-}$ *15 weeks HFD* condition: $p< 0.0001$, *post hoc*Sidak test, n=5) (Figure 3.3.2).

At the time-point of 15 weeks HFD, the proteins associated to ER stress response in NURP1$^{-/-}$ HFD mice had a similar expression trends reported at the time-point of 10 weeks HFD. Interesting a small increment of both CHOP and BIP protein expression levels has been detected in Nupr1 $^{-/-}$ 15 weeks HFD mice by western blot analysis (Figure 3.3.2).

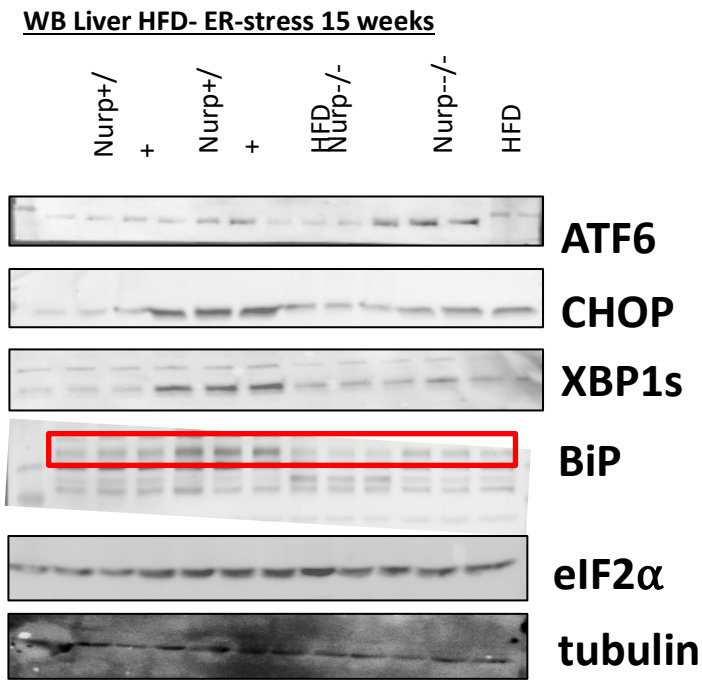

Figure 3.3.2 UPR associated proteins Western blots in NUPR1$^{-/-}$ and NUPR1 $^{+/+}$ 15 weeks HFD and ND control mice

Real time-qPCR analysis were performed to evaluate the expression levels of the major UPR associated genes at the time-point of 15 weeks of HFD. Data have been reported as means ± SEM.

In the figure 3.3.3 we reported the mRNA expression levels of the following ER stress response, UPR associated genes: ATF4, ATF6, CHOP, GADD34, XBP1s, and XBP1u.

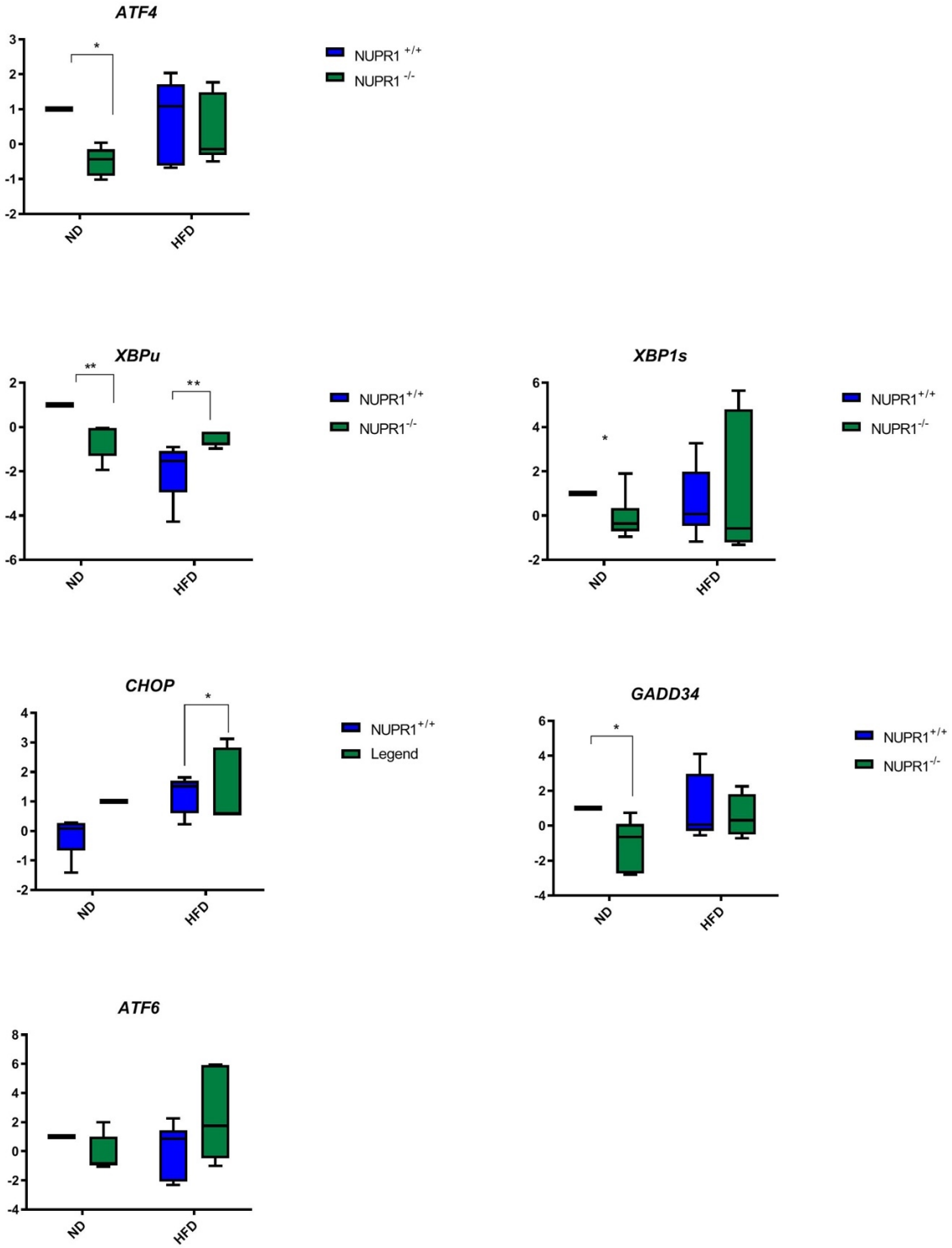

3.3.3. Figure UPR associated genes RT-qPCR in NUPR1-/- and NUPR1 +/+ 15 weeks HFD and ND control mice.

RT-qPCR analysis showed that liver mRNA of ATF4 is downregulated in *NUPR1*$^{-/-}$ compared to *NUPR1*$^{+/+}$ 15 weeks HFD mice (n=5). Two-way ANOVA analysis revealed a significant effect of the genotype (*NUPR1*$^{+/+}$vs *NUPR1*$^{-/-}$ HFD 15 weeks p=0.0295). However no significant effect of diet (p=*0.4152*), as well as interaction between the two factors (p=0.0679) have been observed. Subsequent multiple comparisons uncovered a significant difference between *NUPR1*$^{+/+}$ and *NUPR1*$^{-/-}$ HFD 15 weeks mice (p<0.0185, *post hoc*Sidak test). CHOP mRNA level increased in *NUPR1*$^{-/-}$ compared to *NUPR1*$^{+/+}$ HFD 15weeks mice (n=5). The two-way ANOVA analysis revealed a significant effect of diet (p= 0,0197). However no significant effect of genotype (p=0,2243) as well as interaction between the two factors (p=0,0679mice) have been observed. Subsequent multiple comparisons uncovered a significant difference between *NUPR1*$^{+/+}$ and *NUPR1*$^{-/-}$ HFD 15 weeks mice (p<0.0185, *post hoc*Sidak test). The GADD34 mRNA was upregulated in Nupr1 -/- compared to *NUPR1*$^{+/+}$ HFD 15 weeks mice (n=5). The two-way ANOVA analysis revealed a significant effect of genotype (p= 0.0495). However no significant effect of diet (p=0.1775) as well as interaction between the two factors (p=0.218) have been observed. Subsequent multiple comparisons uncovered a significant difference between *NUPR1*$^{+/+}$ and *NUPR1*$^{-/-}$ HFD 15 weeks mice compared to *NUPR1*$^{+/+}$ HFD 15 weeks mice (p<0.01, *post hoc*Sidak test). The mRNA expression level of ATF6 significantly increased in NURP1-/- compared with NURP1+/+ HFD 15 weeks (effect of diet: p=*0.02926*; effect of genotype p<0.0001; interaction p=0.00381; *NUPR1*$^{+/+}$ vs *NUPR1*$^{-/-}$ HFD 15 weeks: p<0.0001, *post hoc*Sidak test, n=5).

A not significant increment of XBP1s mRNA and a significant difference of XBP1u mRNA levels have been also detected in *NUPR1*$^{-/-}$ compared to *NUPR1*$^{+/+}$ HFD 15 weeks mice (n=5) (effect of diet: p=0.0012; effect of genotype p=0.0023; interaction p=0.0012; *NUPR1*$^{+/+}$ vs *NUPR1*$^{-/-}$ HFD 15 weeks: p=0.0035 *post hoc*Sidak test).

In the figure 3.3.4 we reported the mRNA expression levels of the additional following ER stress response genes: BIP, HyOu (hypoxia up-regulated 1), ERDJ4 (DNAJB9 DnaJ heat shock protein family (Hsp40) member B9), HYOU (Hypoxia Up-Regulated 1), GRP94 (HSP90-Like Protein Chaperone).

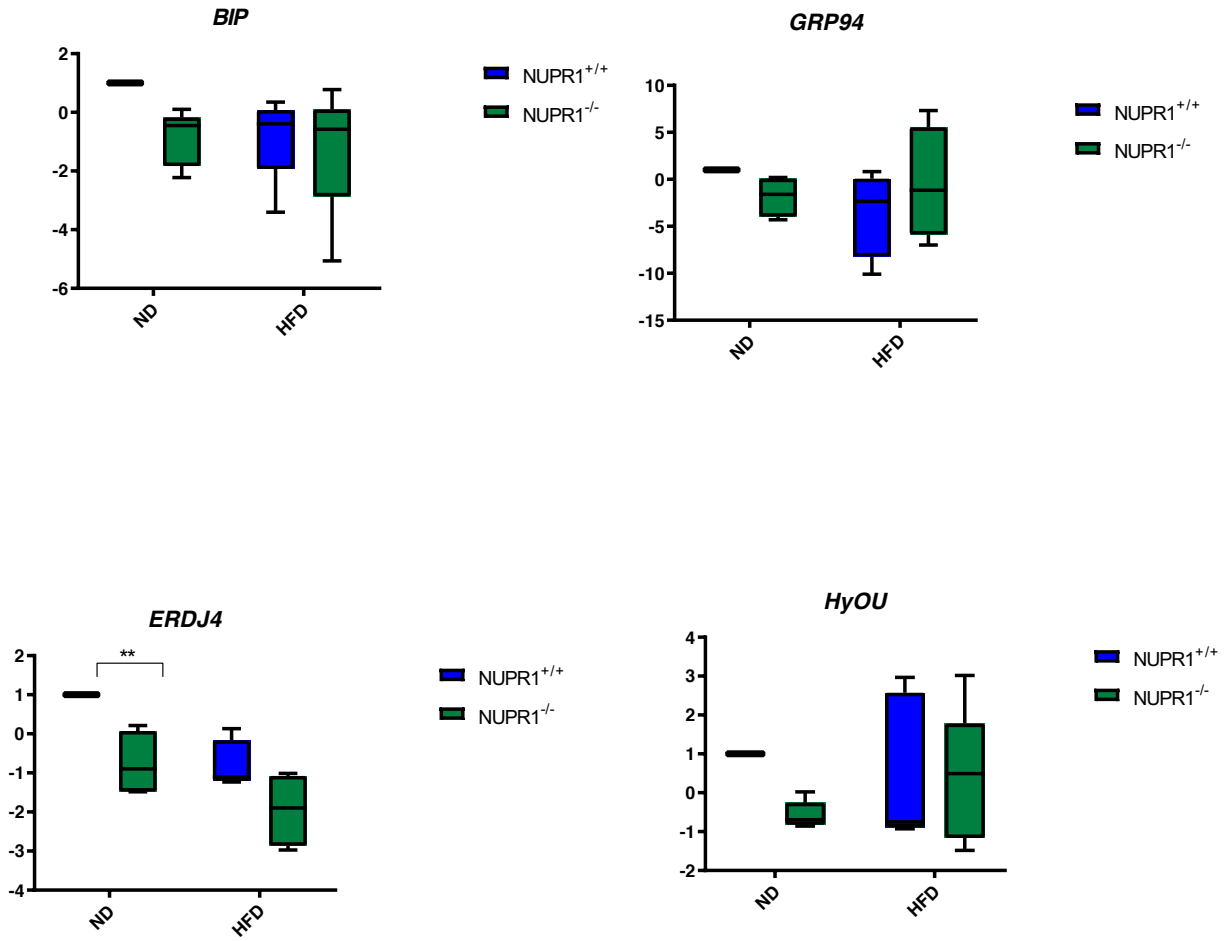

Figure 3.3.4. ER stress response genes RT-qPCR in NUPR1-/- and NUPR1 +/+ 15 weeks HFD and ND control mice.

The expression level of the ER stress response gene BiP was not significantly increased in *NUPR1*$^{-/-}$ compared to *NUPR1*$^{+/+}$ mice HFD 15 weeks mice (n=5). Similarly, the expression of the mRNA of GRP94 was also upregulated in *NUPR1*$^{-/-}$ compared to *NUPR1*$^{+/+}$ HFD mice 15 weeks (n=5). Conversely a not significant downregulation of HyOu mRNA and a significant decrease of ERDj4 mRNA level have been also detected in *NUPR1*$^{-/-}$ compared to *NUPR1*$^{+/+}$ HFD 15 weeks mice (n=5) (effect of diet: p=0.0012; effect of genotype p=0.0016; interaction p=0.3827; *NUPR1*$^{+/+}$ vs *NUPR1*$^{-/-}$ HFD 15 weeks: p=0.0032 *post hoc*Sidak test).

In the figure 3.3.5 we reported the mRNA expression levels of the following metabolic pathways genes: SREBP1C (central lipogenic regulator-sterol regulatory element binding protein), APOB (apolipoprotein B), ChREBP or MLXIPL (MLX interacting protein like), LCAD (Long chain acly-CoA dehydrogenase), MCAD (Medium chain acyl-CoA dehydrogenase deficiency), MTTP (microsomal triglyceride transfer protein), LCB3 (Long-chain base-1-phosphate phosphatase), MCT4 (Monocarboxylate transporters).

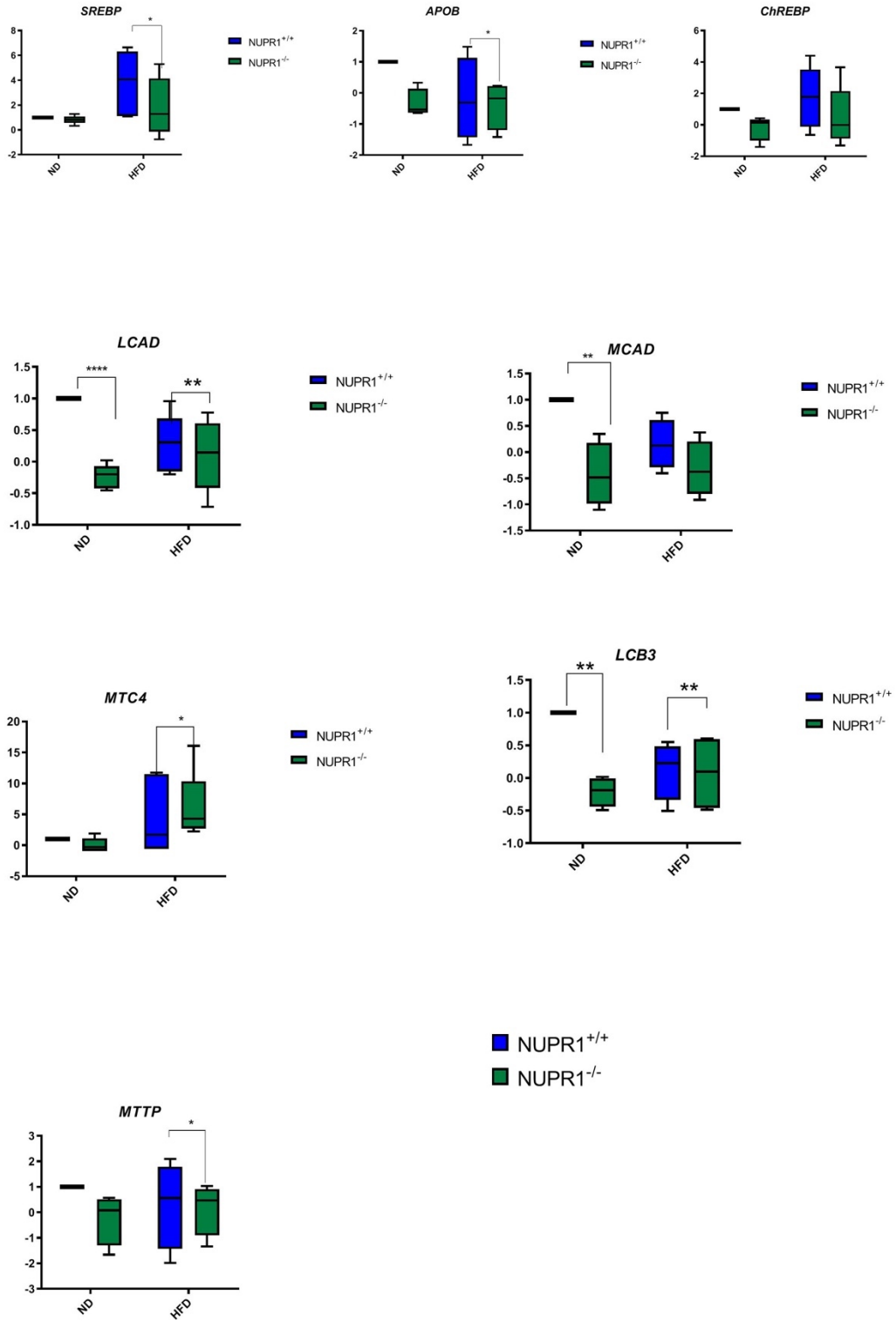

Figure 3.3.5. Metabolic pathways genes RT-qPCR in NUPR1$^{-/-}$ and NUPR1$^{+/+}$ 15 weeks HFD and ND control mice.

The SREBP1C mRNA resulted down-regulated in *NUPR1*$^{-/-}$ compared to *NUPR1*$^{+/+}$ HFD mice 15 weeks (n=5). Two-way ANOVA analysis revealed a significant effect of the diet (*NUPR1*$^{+/+}$vs *NUPR1*$^{-/-}$ HFD 15 weeks p=0.0279). However no significant effect of genotype (p=*0.20*) as well as interaction between the two factors (p=0.28) has been observed.

Both APOB and ChREBP mRNA levels were not significantly decreased in *NUPR1*$^{-/-}$ compared to *NUPR1*$^{+/+}$ HFD mice 15 weeks (n=5).

The LCAD mRNA was significantly down-regulated in *NUPR1*$^{-/-}$ compared to *NUPR1*$^{+/+}$ HFD mice 15 weeks (n=5). Two-way ANOVA analysis revealed a significant effect of the genotype (*NUPR1*$^{+/+}$vs *NUPR1*$^{-/-}$ HFD 15 weeks p=0.0008) as well as interaction between the two factors (p=0.0062). However no significant effect of diet (p=*0.2737*) has been observed. Subsequent multiple comparisons uncovered a significant difference between *NUPR1*$^{+/+}$ and *NUPR1*$^{-/-}$ HFD 15 weeks mice (p=0.0002, *post hoc*Sidak test).

Accordingly, MCAD mRNA expression level was significantly lower in *NUPR1*$^{-/-}$ compared to *NUPR1*$^{+/+}$ HFD mice 15 weeks (n=5) (effect of diet: p<0.0001; effect of genotype p=0.0016; interaction p< 0.0001; *NUPR1*$^{+/+}$ and *NUPR1*$^{-/-}$ *HFD* mice 15 weeks: p<0.0001, *post hoc*Sidak test).

MTTP mRNA expression was downregulated in *NUPR1*$^{-/-}$ compared to *NUPR1*$^{+/+}$ HFD mice 15 weeks (n=5), but the difference trends did not reach statistical significance.

A significant downregulation has been reported for MCT4 in NUPR1$^{-/-}$ compared to *NUPR1*$^{+/+}$ HFD mice 15 weeks (effect of diet: p = 0.0002; effect of genotype p<0.0001; interaction p<0.0001; *NUPR1*$^{+/+}$ vs *NUPR1*$^{-/-}$ mice 15 weeks: p<0.0001, *post hoc*Sidak test, n=5).

Conversely the LCB3 expression mRNA level was significantly increased in NUPR1$^{-/-}$ compared to *NUPR1*$^{+/+}$ HFD mice 15 weeks. The two-way ANOVA analysis revealed a significant effect of genotype (p<0.0070) and interaction (p<0.0109). However no significant effect of diet (p=0.1560) has been observed. Subsequent multiple comparisons uncovered a significant difference between *NUPR1*$^{+/+}$ and *NUPR1*$^{-/-}$ HFD 15 weeks mice (p<0.001, *post hoc*Sidak test), limited to control conditions.

In the figure 3.3.6 we reported the mRNA expression levels of the following additional metabolic pathways genes: PPARalpha (peroxisome proliferator activated receptor alpha), CPT-1A (carnitine palmitoyltransferase-1a), CPT-1b (carnitine palmitoyltransferase-1b), ACC (acetyl-CoA carboxylase), PGK1 (phosphoglycerate kinase 1), ACLY (ATP citrate lyase), SCD1 (Stearoyl-CoA desaturase).

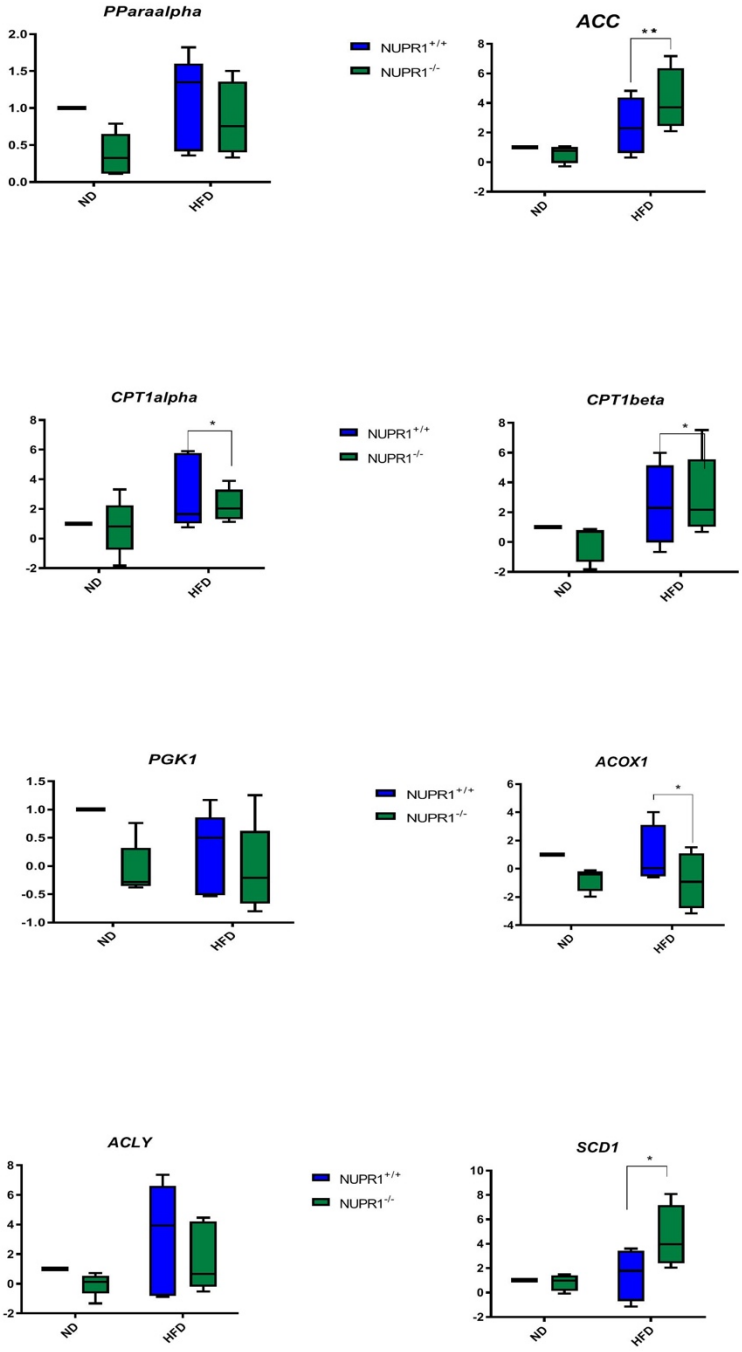

Figure 3.3.6. Metabolic pathways genes RT-qPCR in NUPR1$^{-/-}$ and NUPR1 $^{+/+}$ 15 weeks HFD and ND control mice.

The PPARα expression level was significantly downregulated in NUPR1$^{-/-}$ compared to *NUPR1*$^{+/+}$ HFD 15 weeks mice (n=5). Two-way ANOVA analysis revealed a significant effect of the genotype (*NUPR1*$^{+/+}$vs *NUPR1*$^{-/-}$ HFD 15 weeks p=0.0315). However no significant effect of diet (p=*0.1515*), as well as interaction between the two factors (p=0.2146) have been observed. Subsequent multiple comparisons uncovered a significant difference between *NUPR1*$^{+/+}$ and *NUPR1*$^{-/-}$ HFD 15 weeks mice (p<0.0391, *post hoc*Sidak test).

The expression levels of CPT1-A and the CPT1-b proteins were significantly lower in *NUPR1*$^{-/-}$ compared with the *NUPR1*$^{+/+}$ HFD 15 weeks mice (n=5) (CPT1-A: effect of diet: p=0.00286; effect of genotype p<0.0001; interaction p<0.0001); (CPT-1b: effect of diet: p=0.0121; effect of genotype p<0.0001; interaction p< 0.0001) However subsequent multiple comparisons showed a not significant difference between *NUPR1*$^{+/+}$ and *NUPR1*$^{-/-}$ HFD 15 weeks mice (p=0.70; p=0.88, *post hoc*Sidak test). CPT1-A and the CPT1-b proteins controls mitochondrial beta-oxidation and are inhibited by malonyl-CoA, the product of acetyl-CoA carboxylase (ACC), that in our analysis resulted significantly up-regulated in *NUPR1*$^{-/-}$ compared with the *NUPR1*$^{+/+}$ HFD 15 weeks mice (n = 5) (effect of diet: p=0.00054; effect of genotype p<0.0001; interaction p < 0.0001). However subsequent multiple comparisons showed a not significant difference between *NUPR1*$^{+/+}$ and *NUPR1*$^{-/-}$ HFD 15 weeks mice (p=0.23, *post hoc*Sidak test).

We reveled a significant down-regulation of ACOx1 expression in *NUPR1*$^{-/-}$ compared with the *NUPR1*$^{+/+}$ HFD 15 weeks mice (n=5) (effect of diet: p<0.0001; effect of genotype p=0.00048; interaction p<0.0001). However subsequent multiple comparisons showed a not significant difference between *NUPR1*$^{+/+}$ and *NUPR1*$^{-/-}$ HFD 15 weeks mice (p=0.174, *post hoc*Sidak test).

Phosphoglycerate kinase (PGK1) is a highly conserved enzyme that is crucial for glycolysis. In our analysis the PGK1 mRNA level was significantly decreased in *NUPR1*$^{-/-}$ compared with the *NUPR1*$^{+/+}$ HFD 15 weeks mice (n=5). Two-way ANOVA analysis revealed a significant effect of the genotype (*NUPR1*$^{+/+}$vs *NUPR1*$^{-/-}$ HFD 15 weeks p=0.0201). However no significant effect of diet (p=*0.1744*), as well as interaction between the two factors (p=0.1624) have been observed. Subsequent multiple comparisons uncovered a significant difference between *NUPR1*$^{+/+}$ and *NUPR1*$^{-/-}$ HFD 15 weeks mice (p=0.0226, *post hoc*Sidak test).

Similarly the ACLY mRNA level was not significantly down-regulated in *NUPR1*$^{-/-}$ compared with the *NUPR1*$^{+/+}$ HFD 15 weeks mice (n=5).

Conversely the stearoyl-CoA desaturase 1 (SCD1) mRNA was significantly upregulated in in *NUPR1*$^{-/-}$ compared with the *NUPR1*$^{+/+}$ HFD 15 weeks mice (n=5). Two-way ANOVA analysis revealed a significant effect of the diet (*NUPR1*$^{+/+}$vs *NUPR1*$^{-/-}$ HFD 15 weeks p=0.0318). However no significant effect of genotype (p=*0.12*), as well as interaction between the two factors (p=0.09) have been observed. Subsequent multiple comparisons uncovered a not significant difference between *NUPR1*$^{+/+}$ and *NUPR1*$^{-/-}$ HFD 15 weeks mice (p<0.0871, *post hoc*Sidak test).

In the figure 3.3.7 we reported the mRNA expression levels of the following additional metabolic pathways genes: Acox1(Fatty acyl-coenzyme A oxidase 1), FAS/FANS (Fatty Acid Synthase), DGAT1acyl-CoA (diacylglycerol acyltransferase-1), DGAT2 acyl-CoA (diacylglycerol acyltransferase-2), FABP1 (FATTY ACID binding protein), SCL27α (Fatty acid transporter proteins family) also known as FATP1, ADFP (Perilipin 2 (Plin2).

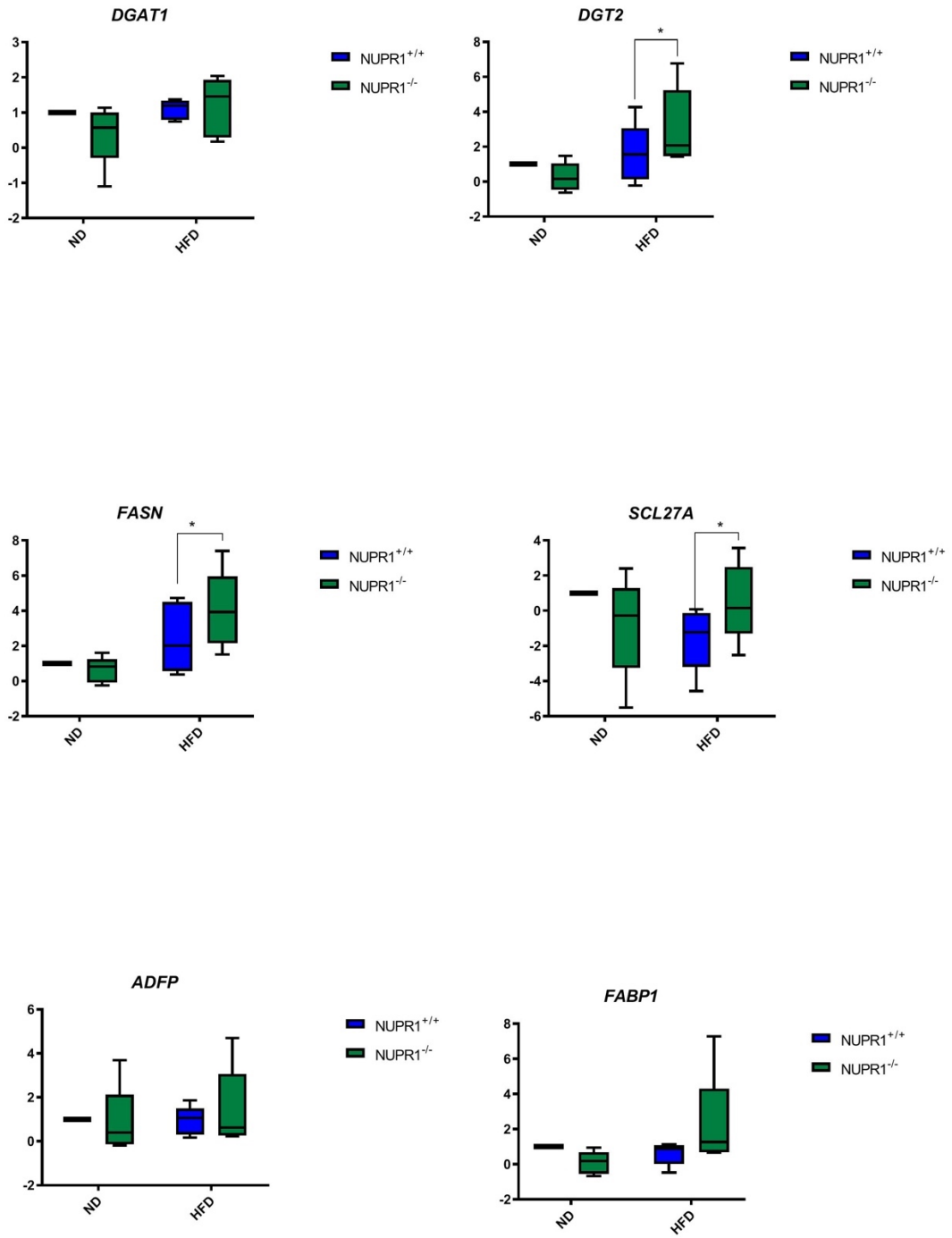

Figure 3.3.7. Metabolic pathways genes RT-qPCR in NUPR1-/- and NUPR1 +/+ 15 weeks HFD and ND control mice.

The Dgat 1 and Dgat 2 mRNA were significantly upregulated in *NUPR1*$^{-/-}$ compared with the *NUPR1*$^{+/+}$ HFD 15 weeks mice (n=5) (effect of diet *p*=0,0197; effect of genotype *p*<0.0001; interaction p = 0.0002; *NUPR1*$^{+/+}$ vs *NUPR1*$^{-/-}$ in HFD 15 weeks condition: *p*<0.0001 *post hoc*Sidak test).
The expression of FASN mRNA was significantly increased in *NUPR1*$^{-/-}$ compared with the *NUPR1*$^{+/+}$ HFD 15 weeks mice (n=5) (effect of diet *p*= 0.0028; effect of genotype *p*<0.0002; interaction p = 0.0002; *NUPR1*$^{+/+}$ vs *NUPR1*$^{-/-}$ HFD 15 weeks mice: *p*<0.0001 *post hoc*Sidak test).
Similarly the SLC27α mRNA was significantly upregulated in NUPR1-/- compared with the NUPR1+/+ HFD 15 weeks mice (n=5), (effect of diet p= 0.0028; effect of genotype p<0.0002; interaction p=0.0479; NUPR1+/+ vs NUPR1-/- HFD 15 weeks mice: p<0.0001 post hocSidak test).
Finally a not significant decrease of ADFP mRNA along with an increase of FABP have been reported in *NUPR1*$^{-/-}$ compared with the *NUPR1*$^{+/+}$ HFD 15 weeks mice (n=5).

3.4. NUPR 1 AND STEATOHEPATITIS.

Hepatocytes perform a myriad of metabolic functions, including plasma protein synthesis and secretion, lipoprotein and very low density lipoprotein (VLDL) assembly and secretion, cholesterol biosynthesis, and xenobiotic metabolism, and thus are enriched in both smooth and rough ER. These metabolic functions and their compartmentalization in the ER have been long recognized; however, it is not known how ER homeostasis and signaling through the UPR sensors impact these diverse ER functions. Perturbations in ER homeostasis leading to dysfunction and activation of some of the UPR sensors occur in several liver diseases. Depicted herein are the stimuli that can lead to ER dysfunction. Steatosis occurs in the liver following both acute and chronic liver diseases. Hepatocellular injury often results in an increase of serum ALT levels and serum ALT levels can be used as a marker for liver injury. (83)Alanine Aminotransferase (ALT), also known as serum glutamic-pyruvic transaminase (SGPT), is a pyridoxal-phosphate-dependent enzyme that catalyzes the reversible transfer of an amino group from alanine to α-ketoglutarate, generating pyruvate and glutamate. ALT is found primarily in liver and serum. We tested the serum ALT activity level in NUPR1$^{-/-}$ and NUPR1$^{+/+}$ normal feed control mice, HFD 15 weeks mice, and 16h post Tun injections. As shown in figure 3.4.1 there was a not significant increase of serum ALT activity in the Nupr1$^{-/-}$ compared to Nupr1$^{+/+}$ HFD 15 weeks mice. Moreover the level of serum ALT activity was significantly increased in the Nupr$^{-/-}$ compared to Nupr1+/+ mice after 16h of Tu injections (p<0.001). The increased levels of serum ALT activity was consistent with the severity of steatohepatitis, suggesting that NUPR1 plays a role in the prevention of lipotoxicity and liver steatosis.

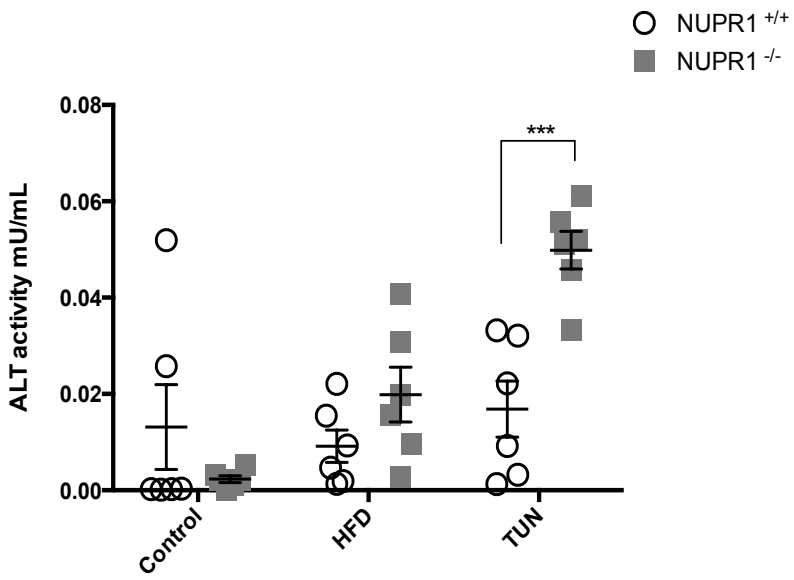

Figure 3.4.1. Serum ALT levels in the Nupr1-/- and Nupr1+/+ mouse serum NF, HFD and after Tunicamicyn injections.

In the figure 3.4.2 is shown the HE and Oil Red O stains of the liver tissue of NUPR1$^{+/+}$ and NUPR1$^{+/+}$ HFD 15 weeks mice. The histological analysis of the liver specimens revealed that Nupr1$^{+/+}$ HFD mice had minimal focal inflammation, minimal perisinusoidal fibrosis, and no signs of steatosis, while Nupr1$^{-/-}$ HFD mice had mild focal inflammation with focal steatosis, and perisinusoidal fibrosis.

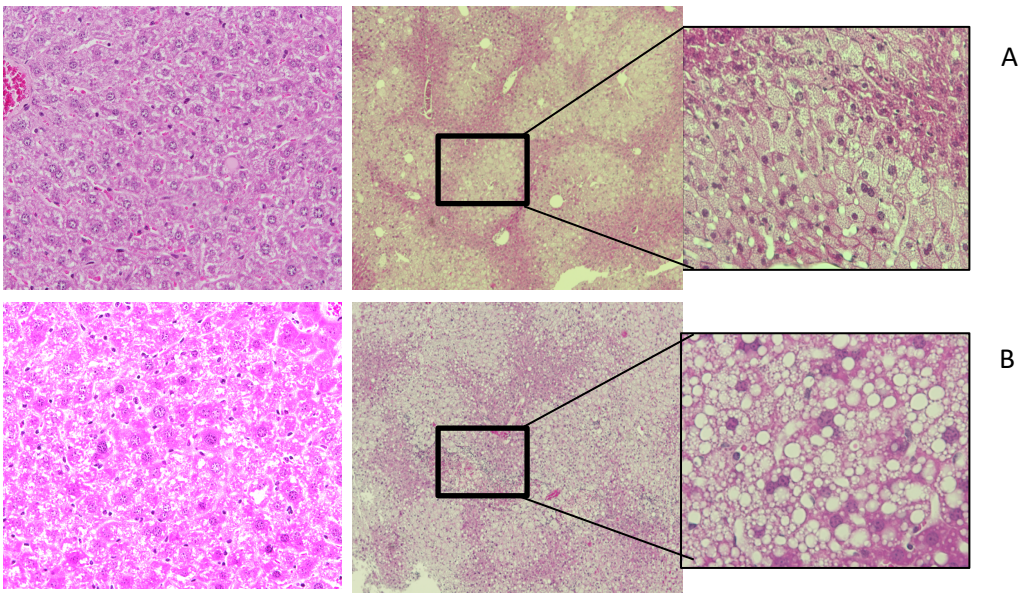

Figure 3.4.2. Pathological changes by H&E staining in: A) NUPR1$^{+/+}$ and B) NUPR1$^{-/-}$ HFD 15 weeks

CHAPTER 4

Discussion 4

Cancer, cardiovascular diseases, metabolic disorders (including obesity, different type of diabetes and non-alcoholic fatty liver disease) appear to share certain pathological traits such as intracellular stress and inflammation induced by metabolic disturbance stemmed from over nutrition frequently aggravated by a modern, sedentary life style. (84)(85)
The evidence that ER stress is involved in the pathogenesis of metabolic pathologies has grown during the last few years, and the number of diseases involving ER stress has also increased, with many of them bearing similar molecular manifestations of oxidative stress, inflammation, and lipotoxicity. The UPR rescues the cells from damage caused by ER stress, and in case of persistent stress, the UPR induces apoptosis to eliminate cells with unresolvable stress. (86)
We investigated the role of NUPR1 in ER physiological cellular stress in vivo models and its relationships with some pivotal genes which act as major players of metabolic cell functions and disorders.

In this work we first reproduced the “acute” ER stress conditions by tunicamycin injection, to confirm that NUPR1-deficient mice are unable to activate the ER stress response. The results of the Western Blot analysis showed that NUPR1-deficient status was associated to a decrease of the major UPR associated proteins (e.g. ATF4, CHOP, BIP), while normal levels of eif2alfa and p-PERK have been detected, overall suggesting that NUPR1 could act downstream of PERK within the UPR complex. Therefore the absence of NUPR1 led to an inefficient activation of the PERK branch of the ER stress response.

Thereafter we reproduced the “chronic” ER stress conditions by HFD, to confirm that NUPR1-deficient mice are unable to activate the ER stress response. The results of both Western blots and RT-qPCR analysis after 10 weeks HFD showed the downregulation of BIP, XBP1, and of the following pro-apoptotic factors, ATF4, CHOP and GADD34 in *NUPR1*$^{-/-}$ mice, confirming that also in physiological ER stress conditions, NUPR1 act downstream of the PERK branch within the UPR complex playing a crucial role in the activation of ER stress response pathways.

To study whether the lack of NUPR1 is stored over the times and to understand the specific molecular mechanisms underlying such alterations in the physio-pathologic status of ER stress, we examined hepatic genes differentially expressed after a long-term (15 weeks) high-fat intake in *NUPR1* wild-type (*NUPR1*$^{+/+}$) mice and NUPR1 knockout (*NUPR1*$^{-/-}$) compared with their respectively normal chow diet (ND) controls. Western blot for the major UPR associated proteins in NURP1-/- mice at 15 weeks HFD showed similar expression trends reported at the time-point of 10 weeks. Interesting western blot analysis at 15 weeks showed a further small increment of both CHOP and BIP protein expression levels in Nupr1 deficient mice. Differently from what observed at 10 weeks, the relative 15 weeks RT-qPCR analysis showed an upregulation of XBP1, CHOP, and BIP mRNAs, likely attributable to the very wide range of mRNA levels detected in the tested mice. A potential biological explanation to this phenomena could be provided by the parallel activation of other signaling pathways under a prolonged HDF condition, ultimately replacing the role of NUPR1 in the

chronic ER stress response. Of note it has been reported in literature that the stimulation of BiP mRNA or protein expression with exercise could be related to the training protocols, animal model, tissues analyzed or health status(87). The ERdj4a is a member of HSP40 chaperon, localized in the ER, which was associated to the misfolded protein ER stress (88). The HyOu works in concert to BIP to ensure the correct folding of proteins targeted for extracellular secretion (89). Both HyOu and ERDj4 mRNA resulted down-regulated in absence of NUPR1-/-, thus failing to activate an effective UPR response.

In the liver the chronic ER stress has been associated to a pathological condition characterized by lipid accumulation, named lipotoxicity, which is often accompanied by the transcriptional suppression of several metabolic genes(90). To unraveling the potential role of NUPR1 in the development of liver steatosis, we decide to analyze also the transcriptomics profile of the major metabolic pathways genes.

Among the multiple analyzed genes, we reported a down-regulation of the majority mRNA associated to lipogenesis (SREBP, ACLY, ChREBP) and lipoprotein (APOB, PPAR-alfa, MTTP) in *NUPR1* deficient mice. Both LCAD and MCAD fatty acid metabolisms mRNA were also downregulated, as consequence of PPAR-alfa deficit. Similarly beta-oxidation mRNA ACOX1 and CPT1-alfa, as well as MTC4 and PGK1 were downregulated in $NUPR1^{-/-}$ compared to $NUPR1^{+/+}$ HFD mice 15 weeks.

The sterol regulatory binding protein (SREBP) transcription factors are the master regulators of triglyceride and cholesterol synthesis in hepatocytes, and are essential for obesity and alcohol induced steatosis. In some cells, UPR activation causes SREBP activation whereas in others, SREBP expression, activation or function is suppressed by ER stress. Whether activation of the UPR is coupled to SREBP driven steatosis remains to be determined (91). BIP overexpression has been shown to inhibit insulin induced SREBP-1c activation in cultured primary hepatocytes.(92) In our experiments, BIP overexpression has been observed in $NUPR1^{-/-}$ compared to $NUPR1^{+/+}$ HFD mice 15 weeks. However we assessed a downregulation of SREBP1C mRNA levels, suggesting that the lack of Nupr1 is associated to an impaired SREBP activity and ER stress response.

Carbohydrate response element binding protein (ChREBP) is a glucose-sensing transcription factor that mediates the induction of glycolytic and lipogenic genes in response to glucose. It acts as one of the master regulators of intracellular glucose metabolism, with a basic helix–loop–helix leucine zipper (bHLH-LZ) transcription factor expressed in liver. (93) Similarly to SREBP, we reported an interesting down-regulation of ChREBP mRNA levels in $NUPR1^{-/-}$ compared to $NUPR1^{+/+}$ HFD 15 weeks mice, suggesting that the lack of Nupr1 is associated to an impaired ChREB activity.

Several works suggested a protective role of APOB against HFD-induced inflammation, insulin resistance, dyslipidemia, and nonalcoholic fatty liver disease, without ameliorating adiposity (94). It is well known that APOB is regulated at translational and post-translational levels, including a number of pathways for intracellular degradation (95). Thus the ER stress–mediated reduction of APOB secretion could represent a link between ER stress and hepatic steatosis.
Our experiments showed a downregulation of APOB in *NUPR1* deficient mice, suggesting a direct or indirect connection between Nupr1 and APOB function in the context of ER stress response and supporting the role of APOB as a prime target for UPR-mediated downregulation.

Microsomal TG transfer protein (MTTP) is required for the assembly and secretion of TG (TG)-rich lipoproteins from both enterocytes and hepatocytes (96). Liver-specific deletion of *MTTP* produced a dramatic reduction in plasma of very low density lipoprotein-TG and virtually eliminated apolipoprotein B100 (apoB100)

secretion (97). The downregulation of MTTP in NUPR1 $^{-/-}$ HFD 15 weeks mice suggested, similarly to APOB, a potential association between the loss of NUPR1 and the decrease of these two mRNA levels.

PPAR-alfa is a member of the nuclear hormone receptor superfamily of ligand-inducible transcription factors. Activation of PPAR-alpha promotes uptake, utilization, and catabolism of fatty acids by upregulation of genes involved in fatty acid transport, fatty acid binding and activation, and peroxisomal and mitochondrial β-oxidation. (98) Interestingly, XBP1s, which is one of the main players of the ER stress response was linked to PPAR-alfa (99). Furthermore NUPR1 is a target for all three PPAR isoforms, which interact with peroxisome proliferator response element in NURP1 promoter. The progressive PPAR-alfa and P8 mediated ER stress contribute to the hepatocarcinogenesis in ACOX -/- mice. (100)
The results of our analysis, showing a downregulation of ACOX1 and PPAR-alfa in NUPR1 deficient mice confirm a relationship between these different factors in modulating the ER stress response.

Clearly, mouse models differ from human disease in many different aspects. Cutoff points such as waist circumference cannot be transferred from humans to mice. In addition, normal mouse lipoprotein profiles have primarily atheroprotective HDL, whereas normal human lipoprotein profiles contain primarily atherogenic low-density lipoproteins (LDL). Finally, the presence of hypertension in obese mice is inconsistent. Thus, no one mouse model can exactly mimic all aspects of human metabolic syndrome. (101)

Previous reports in cultured hepatocytes and other cell types have suggested that ER stress stimulates lipogenesis (102). However, our own work has suggested that important genes of the lipogenic pathway are downregulated by the ER stress in NUPR1 deficient mice. In addition the cytological and histological findings in Nupr1-/- HFD 15 weeks mice showed reduced lipotoxicity effects than expected. Given these findings we speculate that an impaired ER stress UPR-mediated response, as observed in NUPR1 deficient mice, is associated to a reduced lipotoxocity, suggesting a crucial role of NUPR1-mediated ER stress response to the development of liver steatosis.

SCD1 plays a key role in preventing lipotoxic effects, as it converts saturated fatty acids (SFAs) to less harmful monounsaturated fatty acids (103). An increase of intracellular fatty acid metabolites, such as diacylglycerol and ceramides, leads to ER stress and serine/threonine phosphorylation of insulin receptor substrates and the activation of nuclear factor (NF)-κB signaling pathways (104). The FASN pathway produces long-chain fatty acids, combining acetyl-CoA produced from glycolysis with malonyl-CoA. FASN plays a major role in FASN and has been shown to be upregulated in different cancer cells (105).
As previously discussed for the UPR associated genes, the upregulation of these two important fatty acid metabolism genes SCD1 and FASN in Nupr1-/- HFD 15 weeks mice, suggested that the protective role of NUPR1 may be time-dependent, with the activation of other signaling pathways under a prolonged HDF condition (106) which are able to replace NUPR1 in the chronic ER stress response. These findings were unexpected and awaits further studies to explain.

In conclusions the results of this work confirm the crucial role of NUPR1 in the activation of UPR response pathway in physio-pathological ER stress condition suggesting a potential contribution of NUPR1-mediated ER stress response to the development of liver steatosis.

CHAPTER 5

Supplementaries 5

5.1 BUFFERS SOLUTIONS RECEIPTS:

TABLE 5.1.1. Tails lysis buffer. (Final Concentration to 500ml)

Reagents and relative initial Concentration	final Concentration	Final Volume
1M Tris pH 8.0	10mM	5ml
5ml, 5M NaCl	100mM	10ml
0.5M ,EDTA pH 8.0	10mM	10ml
20% SDS	20%	5 mL
dH_20	to 500ml	
Add 20µl of a 20 mg/ml stock per 1ml of tail lysis buffer.		

TABLE 5.1.2. Buffers Used In Western Blot Procedures.

Total volume	Buffer	Components
1L	Running Buffer10x	100 running 10x, 900ddw
1L	TRANSFER BUFFER 10x	tris base 121g,562.5 glycina,5 l ddw
1L	TRANSFER BUFFER 1x	100 transfer buffer 10x, 200mL di ETOH , 700 ddw)
1L	Washing buffer : TBS 1x	100mL in 900mL DDWater
1L	TRANSFER BUFFER 1x TBS –T	0.1 tween 100mL in 900mL DD Water 1mL di TWEEN
1L	Blocking MILK	5% MILK in TBS-t

TABLE 5.1.3. RIPPA BUFFER RECEIPT.

Reagents	Final Concentration
Na deoxycholate10%(	1M
SDS 20%	0.1M
TRITON-X 100 1%	1M
TRIS BASE pH8 ,	2M
NaCl	5M

TABLE 5.1.4**.** RIPA BUFFER WITH A PROTEASE INHIBITOR COCKTAIL (SIGMA) .

Reagents	final Concentration	Final Volume
NaF	1mM,	5µL
Na_3VO_4 ,	100 µM	50 µL
βGlycerol-P,	1 M	200µ L
PMSF 1%,	1mM	50µL
of RIPA	4.670 mL	5 mL

5.2 DNA EXTRACTION , PROCEDURE AND REAGENTS OF PCR END-POINT.

TABLE 5.2.1. Procedure of Genotyping P8 Mice.

<table>
<tr><th>TIMING</th><th>REAGENTS</th><th>EXPOSITION</th></tr>
<tr><td>Day1</td><td>1)to each tails add :250µl of Lisys Buffer contains Proteinase K</td><td>2)in 50-60C water bath overnight</td></tr>
<tr><td rowspan="4">Day2</td><td>3)Spin tubes-
add 500 µl of isopropanol-</td><td rowspan="4">7) Incubate in 50-60C water for some hours</td></tr>
<tr><td>4)recover DNA by centrifuging, max speed</td></tr>
<tr><td>5)Place tubes inverted on bench and allow to air dry 5 minutes,</td></tr>
<tr><td>6)Add 200µl of TE pH 7.5</td></tr>
<tr><td>Day2/3</td><td colspan="2">8)PCR and agar gel</td></tr>
</table>

TABLE 5.2.2. Procedure of Genotyping P8 Mice 5'->3'.

PRIMER	PRIMER SEQUENCE **5'->3'**
KO2B	GGA GGT GTG TGA GGT TAG G
RF51	GGG GCC TGA AGA ACG AGA TCA GC
PRP8-72	GGG TGG TTT AGG GAG GAG ACA
CRE 26	CCT GGA AAA TGC TTC TGT CCG
CRE 36	CAG GGT GTT ATA AGC AAT CCC
$Kras^{G12D}$	GTG TTT CCC CAG CAC AGT GC
$Kras^{G12D}$	CTC TTG CCT ACG CCA CCA GTC C

TABLE 5.2.3. PCR end point Reagents, genotyping P8 mice.

REAGENT	VOLUME
Terra PCR RED DYE premix (2x)	10 µl
MilliQ H_2O	7.9 µl
Primers (20 µM)	0.3 µl
DNA genomic	1.5 µl

TABLE 5.2.4 Termo Cycler Program: PCR end point , genotyping P8 mice.

CYCLES	TEMPERATURE	TIME
INITIAL DENATURATION	98° C	2 MIN
STEPS REPEATED FOR 34 CYCLES	98° C	10 SEC
	60° C	15 SEC
	68° C	1 MIN
FINAL EXTENSION	68° C	1 MIN
HOLD	4° C	∞

DNA GENOTYPES UV-TRANSILLUMINATORS IMMAGINE

Figure 5.2.5. Genotyping P8, Cre, Kras in agarose gel 3% with TBE 0.5X.

5.3.1 ANTIBODIES APPLICATIONS

TABLE 5.3.1: ANTIBODIES USED AND RELATIVES PROCEDURES

Code	**Antibody**	Cross Reaction	Firm	Molecolar Weight	Exposure	Gel %	Diluizion In 5 Ml	Blot	Primary Antibody Wash	Secondary Antibody
CHOP (L63F7) Mouse mAb #2895	**CHOP Mouse mAb**	H;M; R	cell-signaling	27 kDa	overnight 4°	12	raccomandant 1:1000	5%in BSA	1xTBS-Tween20	mouse IgG2a
XBP-1s Antibody #83418	**XBP1 antibody**	H,M	cell-signaling	60 human /55 mouse kDa	overnight 4°	10	raccomandant 1:1000	not fat dry milk 5%in TSB	1xTBS-Tween20	RABBIT (goat anti rabbit)
ATF-4 (D4B8) Rabbit mAb #11815	**ATF4 RABBIT mAb**	H;M; R	cell-signaling	49 kDa	overnight 4°	12	raccomandet 1:1000 (d 1:500)	not fat dry milk 5%in TSB	1xTBS-Tween20	RABBIT (goat anti rabbit)
ATF-6 (D4Z8V) Rabbit mAb #65880	**ATF6 RABBIT mAb**	H,M	cell-signaling	90/100 kDa	overnight 4°	10	raccomandet 1:1000 (d 1:500)	not fat dry milk 5%in TSB	1xTBS-Tween20	RABBIT (goat anti rabbit)
PERK (C33E10) Rabbit mAb #3192	**PERK**	H M R Mk	cell-signaling	140 kDa	overnight 4°	7	raccomandant 1:1000	not fat dry milk 5%in TSB	1xTBS-Tween20	RABBIT (goat anti rabbit)
IRE1α (14C10) Rabbit mAb #3294	**IREα**	H;M; R	cell-signaling	130 kDa	overnight 4°	7	raccomandant 1:1000	not fat dry milk 5%in TSB	1xTBS-Tween20	RABBIT (goat anti rabbit)
BiP (C50B12) Rabbit mAb #3177	**BIP**	H,M	cell-signaling	78 kDa	overnight 4°	10	raccomandant 1:1000	not fat dry milk 5%in TSB	1xTBS-Tween20	RABBIT (goat anti rabbit)
Phospho-eIF2α (Ser51) (D9G8) XP® Rabbit mAb #3398	**P-Eif2α**	H;M; R	cell-signaling	38 kDa	overnight 4°	12	raccomandant 1:1000	not fat dry milk 5%in TSB	1xTBS-Tween20	RABBIT (goat anti rabbit)
eIF2α Antibody #9722	**Eif2α**	H;M; R	cell-signaling	36 kda	overnight 4°	12	raccomandant 1:1000	5%in BSA	1xTBS-Tween20	RABBIT (goat anti rabbit)
Phospho-PERK (Thr980) (16F8) Rabbit mAb #3179	**p-PERK**	R	cell-signaling	170 kDa	overnight 4°	7	raccomandet 1:1000 (d 1:500)	5%in BSA	1xTBS-Tween20	RABBIT (goat anti rabbit)

5.4 RNA EXTRACTION AND AMPLIFICATION (Reverse Transcriptase)

TABLE 5.4.1. Total RNA isolation from free or frozen liver tissue.

Starting material	**Quantity**	**RNA yield**
LIVER	**1 mg**	**6-10µg**

TABLE 5.4.2. Equipments to total RNA isolation.

Equipments : RNA isolation	
Homogenizator	**Precellys or Tissue Tearor Homogenizer**
Centrifuge and rotor capable of reaching 12.000xg and 4°	**thermofisher**
Polypropylene micrcentrifuge tubes	**thermofisher**
RNase ZAP	**Cat #AM9780**

TABLE 5.4.3 Reagents to total RNA isolation.

Reagents: RNA isolation	**For 1 sample(50-100mg of free tissue)**
Ethanol 75%	**1 mL**
Chloroform	**0.2 mL**
Isopropanol	**0.5 mL**
RNA free water of 0.5% SDS	**20-50 µl**
TRIZOL	**1 mL**

TABLE 5.4.4 RNA yield

Method	Procedure
Absorbance 260 nm	**Calculate the Rna concentration using the formula** **A260xdilutionx40=µg RNA/ mL** **Procedure :Microplate Spectrophotometer (Epoch BioTek)**

TABLE 5.4.5. First strand cDNA Synthesis: GoScript Reverse Trascriptase. (PROMEGA CAT#.A5001)

Reagents	Final volume
Experimental RNA (up to 5 µg/ reaction)	(1000 µg/mL) 1 µL
Primer oligo$(dT)_{15}$ (up to 5 µg/ reaction)	1 µL
Nuclease free water	to final volume
Final volume	5 µL
Placed tubes into a preheated 70° heat block for 5 min.	

TABLE 5.4.6 Reverse transcription reaction mix GoScript Reverse Transcriptase. (PROMEGA CAT#.A5001)

Reagents	Final volume
Go Script™ 5x Reaction Buffer	4µL
$MgCl_2$ (1.5-5.0 mM)	1.2-6.4µL
PCR Nucleotide mix	1µL
Recombinant RNasin ribonuclease inhibitor	20u
Go Script™ Reverse Transcriptase	1µL
Nuclease free water	Add to final volume
Final volume **15µL**	

TABLE 5.4.7 Termo Cycler Program , Reverse Transcriptase

Cycles	Temperature	Time
Anneal	25°	5 min
Extend	42°C The extension temperature may be optimized between 37°C and 55°C.	up to 60 min
Inactivate Reverse Transcriptase:	70°C	15 minutes.

5.5 REALTIME-qPCR

TABLE 5.5.1 Reagents RT-qPCR

Reagents	For each seample
Go-Taq qPCRMaster Mix	5 μL
CXR Reference Dye	0,1 μL
free water	2.5μL
primers (fw and rev)	0,2 μL

5.5.2. Sequences of RT-PCR primers

mATF4 fw 5′ ACTATCTGGAGGTGGCCAAG-3′
rev 5′CATCCAACGTGGTCAAGAGC-3′

mATF6 fw-5′CAGTTGCTCCATCTCCTCTCC-3′
rev-5′TGGGACACTGGCATTGGTTTG-3′

mChop fw 5′ -CTGCCTTT CACCTTGGAGAC-3
rev-5′CGTTTCCTGGGGATGA-GATA-3

mERdj4 fw-5-CTTGTGCCTTTGGCCACTG;3′
rev-5′-CAC-AGAGTGGCATGTCACCC3′

mXBP1s fw-5′-ACACGCTTGGGAATGGACAC-3′
rev-5′CCATGGGAAGATGTTCTGGG-3′

mXBP1u fw-5′-CCTGAGCCCGGAGGAGAA-3′
rev 5′-CTCGAGCAGTCTGCGCTG-3′

mGRP94:fw 5′-GGGAGGTCACCTTCAAGTCG
rev 3′-CTCGAGGTGCAGATGTGGG

mGRP78 f w-5-CACGTCCAACCCCGAGAA-3′
rev-3-AT-TCCAAGTGCGTCCGATG

mRFLO fw 5′-AGATTCGGGATATGCTGTTGGC-3′
rev 5′-TCGGGTCCTAGACCAGTGTTC-3′

mPPARα fw 5′-GGGCTCCGAGGGCTCTGTCA-3′
rev 5′-TGCAGCTCCGATCACACTTGTCG-

mMCAD fw 5′-GGATGACGGAGCCAATG-3′
rev 5′-GGGTGTCGGCTTCCACAATG-3′

mLCAD fw 5′-GACGGCGGGCAAGTGTATC-3
rev 5′-GCAGGCGATCGAGCTTCAC-

mFasn fw 5′-TCC ACC TTT AAG TTG CCC TG-3′
rev 5′-TCT GCT CTC GTC ATG TCA CC-3′;

mAcox1 fw 5′-TTA AAC ACC CAC CCA CCA AG-3′,
rev 5′-CGA AAG CCT GGA GGT AAA GA-3′;

mScd1 fw 5′-TTCCGCCACT CGCCTACA 3′,
rev 5′-CTTTCCCAGTGCTGAGATCGA-3′;

mSrebp1c fw 5′-CATCGACTACATCCGCTTCTTG-3′,
rev -5′-TTTTGTGTGCACTTCGTAGGGT-3′;

mCPT1 fw 5′-AGA ATC TCA TTG GCC ACC AG-3′,
rev -5′-CAG GGT CTC ACT CTC CTT GC-3′;

mDGAT1 fw 5′-TCCGCCTCTGGGCATTC 3′;
rev-5′, GAATCGGCCCACAATCCA3′;

fw-mDGAT2, GCTGAGTCCCTGAGCTCCAT;3′
rev-5′ CACAAAGCCTTTGCGGTTCT3′;

TABLE 5.5.3. Termo Cycler Program RTqPCR

Cycles	Temperature	Time
hold	95°	1 min
40 cycles	95°C	20 seconds
	60°	15 seconds
hold	72°	15 min

CHAPTER 6

Bibliography

1. Igarashi T. Cloning and characterization of the Xenopus laevis p8 gene. Dev Growth Differ. 2001 . PMID:11737149
2. Mallo GV. Cloning and expression of the rat p8 cDNA, a new gene activated in pancreas during the acute phase of pancreatitis, pancreatic development, and regeneration, and which promotes cellular growth. J Biol Chem. 1997 PMID: 9405444.
3. Iovanna JL. Expression of the stress-associated protein p8 is a requisite for tumor development. Review Article. Int J Gastrointest Cancer. 2002. PMID:12622419
4. Li Q. Molecular characterization and expression of As-nurp1 gene from Artemia sinica during development and in response to salinity and temperature stress. Biol Bull. 2012. PMID: 22815367
5. Encinar JA . Human p8 is a HMG-I/Y-like protein with DNA binding activity enhanced by phosphorylation. J Biol Chem. 2001.PMID: 11056169
6. Iovanna JL. Expression of the stress-associated protein p8 is a requisite for tumor development. Review Article. Int J Gastrointest Cancer. 2002. PMID: 12622419
7. García-Montero AC. Transforming growth factor beta-1 enhances Smad transcriptional activity through activation of p8 gene expression. Biochem J. 2001.PMID: 11415456PMCID: PMC1221948.
8. Pouponnot C. Physical and functional interaction of SMADs and p300/CBP. J Biol Chem. 1998. (PMID: 9722503)
9. Hoffmeister A. The HMG-I/Y-related protein p8 binds to p300 and Pax2 trans-activation domain-interacting protein to regulate the trans-activation activity of the Pax2A and Pax2B transcription factors on the glucagon gene promoter. J Biol Chem. 2002. (PMID: 11940591)
10. Taïeb D. Inactivation of stress protein p8 increases murine carbon tetrachloride hepatotoxicity via preserved CYP2E1 activity. Hepatology. 2005. (PMID: 15962327)
11. Vasseur S. Mice with targeted disruption of p8 gene show increased sensitivity to lipopolysaccharide and DNA microarray analysis of livers reveals an aberrant gene expression response. BMC Gastroenterol. 2003 (PMID: 12959645)PMCID: PMC212298
12. Carracedo A. The stress-regulated protein p8 mediates cannabinoid-induced apoptosis of tumor cells. Cancer Cell. 2006 PMID: 16616335
13. Nuclear protein p8 is associated with glucose-induced pancreatic beta-cell growth. Diabetes. 2004.PMID: 14749270
14. Goruppi S. Helix-loop-helix protein p8, a transcriptional regulator required for cardiomyocyte hypertrophy and cardiac fibroblast matrix metalloprotease induction. Mol Cell Biol. 2007 (PMID: 17116693) PMCID: PMC1800682.
15. Goruppi S. Signaling pathways and late-onset gene induction associated with renal mesangial cell hypertrophy EMBO J. 2002.PMID: 12374743PMCID: PMC129067
16. García-Montero AC. Transforming growth factor beta-1 enhances Smad transcriptional activity through activation of p8 gene expression. Biochem J. 2001. PMID: 11415456PMCID: PMC1221948

17. Hamidi T. Nupr1-aurora kinase A pathway provides protection against metabolic stress-mediated autophagic-associated cell death. Clin Cancer Res. 2012.PMID: 22899799
18. Hamidi T et al. NUPR1 works against the metabolic stress-induced autophagy-associated cell death in pancreatic cancer cells. J Biol Chem.1997 Dec 19;272(51):32360. PMID: 23047430.
19. Vasseur S. Cloning and expression of the human p8, a nuclear protein with mitogenic activity. Eur J Biochem. 1999.PMID: 10092851
20. Ree AH. Expression of a novel factor in human breast cancer cells with metastatic potential. Cancer Res. 1999 PMID: 10493524
21. Bratland A. Expression of a novel factor, com1, is regulated by 1,25-dihydroxyvitamin D3 in breast cancer cells. Cancer Res. 2000.PMID: 11034106
22. Vasseur S . p8 is critical for tumour development induced by rasV12 mutated protein and E1A oncogene. EMBO Rep. 2002. PMID: 11818333 PMCID: PMC1083964
23. Hamidi T. Nuclear protein 1 promotes pancreatic cancer development and protects cells from stress by inhibiting apoptosis. J Clin Invest. 2012,PMID: 22565310 PMCID: PMC3366404
24. Grasso D. Pivotal Role of the Chromatin Protein Nupr1 in Kras-Induced Senescence and Transformation. Sci Rep. 2015,PMID: 26617245 PMCID: PMC4663475
25. Ma Y, Hendershot LM.J . ER chaperone functions during normal and stress conditions. Chem Neuroanat. 2004 Sep;28(1-2):51-65. Review.PMID:15363491
26. Park SH. Further assembly required: construction and dynamics of the endoplasmic reticulum network. Review Article. EMBO Rep. 2010.PMID: 20559323 PMCID: PMC2897125
27. Niwa M et al. A role for presenilin-1 in nuclear accumulation of Ire1 fragments and induction of the mammalian unfolded protein response. Cell. 1999 Dec 23;99(7):691-702
28. Rutishauser J, Spiess M. Endoplasmic reticulum storage diseases. Swiss Med Wkly. 2002 May 4;132(17-18):211-22 PMID:12087487
29. Wieckowski MR et al. Isolation of mitochondria-associated membranes and mitochondria from animal tissues and cells. Nat Protoc. 2009;4(11):1582-90. doi: 10.1038/nprot.2009.151. Ep ub 2009 Oct 8.PMID:19816421
30. Szegezdi E. Mediators of endoplasmic reticulum stress-induced apoptosis. EMBO Rep. 2006 Sep;7(9):880-5. Review. PMID:16953201
31. Koumenis C et al. Regulation of protein synthesis by hypoxia via activation of the endoplasmic reticulum kinase PERK and phosphorylation of the translation initiation factor eIF2alpha. Mol Cell Biol. 2002 Nov;22(21):7405-16.PMID:12370288
32. Harding HP. Perk is essential for translational regulation and cell survival during the unfolded protein response. Mol Cell. 2000.PMID: 10882126
33. Harding HP et al. Regulated translation initiation controls stress-induced gene expression in mammalian cells. Mol Cell. 2000 Nov;6(5):1099-108.PMID: 11106749
34. Lundgren M et al. Practical management in Wolcott-Rallison syndrome with associated hypothyroidism, neutropenia, and recurrent liver failure: A case report. Clin Case Rep. 2019 May 1;7(6):1133-1138. doi: 10.1002/ccr3.2168. eCollection 2019 Jun. PMID: 31183082
35. Brewer JW1, Diehl JA. PERK mediates cell-cycle exit during the mammalian unfolded protein response. Proc Natl Acad Sci U S A. 2000 Nov 7;97(23):12625-30. PMID: 11035797
36. Lindholm D. ER stress and neurodegenerative diseases. Review Article. Cell Death Differ. 2006 PMID: 16397584
37. Tirasophon W et al. A stress response pathway from the endoplasmic reticulum to the nucleus requires a novel bifunctional protein kinase/endoribonuclease (Ire1p) in mammalian cells. Genes Dev. 1998 Jun 15;12(12):1812-24.PMID:9637683
38. Ron D1, Hubbard SR. How IRE1 reacts to ER stress. Cell. 2008 Jan 11;132(1):24-6. doi: 10.1016/j.cell.2007.12.017.
39. Bertolotti A et al. Dynamic interaction of BiP and ER stress transducers in the unfolded-protein response. Nat Cell Biol. 2000 Jun;2(6):326-32.

40. Lundgren M. Practical management in Wolcott-Rallison syndrome with associated hypothyroidism, neutropenia, and recurrent liver failure: A case report. Clin Case Rep. 2019.PMID: 31183082PMCID: PMC6552956
41. Katayama T. Induction of neuronal death by ER stress in Alzheimer's disease. Review Article. J Chem Neuroanat. 2004 PMID: 15363492
42. Lindholm D. ER stress and neurodegenerative diseases. Review Article. Cell Death Differ. 2006.PMID: 16397584
43. Tirasophon W et al . A stress response pathway from the endoplasmic reticulum to the nucleus requires a novel bifunctional protein kinase/endoribonuclease (Ire1p) in mammalian cells. Genes Dev. 1998 Jun 15;12(12):1812-24.
44. Rutkowski DT1, Kaufman RJ. A trip to the ER: coping with stress. Trends Cell Biol. 2004 PMID:14729177
45. Ladiges WC et al. Pancreatic beta-cell failure and diabetes in mice with a deletion mutation of the endoplasmic reticulum molecular chaperone gene P58IPK. Diabetes. 2005 Apr;54(4):1074-81.
46. Wang XZ et al. Cloning of mammalian Ire1 reveals diversity in the ER stress responses. EMBO J. 1998 Oct 1;17(19):5708-17.PMID:975517
47. Sato N et al. Upregulation of BiP and CHOP by the unfolded-protein response is independent of presenilin expression. Nat Cell Biol. 2000 Dec;2(12):863-70.
48. Nishitoh H et al. ASK1 is essential for JNK/SAPK activation by TRAF2. Mol Cell. 1998 Sep;2(3):389-95.
49. Awad MM et al . Growth regulation via p38 mitogen-activated protein kinase in developing liver. J Biol Chem. 2000 Dec 8;275(49):38716-21PMID:10995779 Davis RJ, 2000
50. Fang Y et al. Biologic behavior and long-term outcomes of breast ductal carcinoma in situ with microinvasion. Oncotarget. 2016 Sep 27;7(39):64182-64190. doi: 10.18632/oncotarget.11639.PMID:27577080
51. Schröder M[1], Kaufman RJ. The mammalian unfolded protein response. Annu Rev Biochem. 2005;74:739-89. PMID: 15952902
52. Wu J. ATF6 alpha optimizes long-term endoplasmic reticulum function to protect cells from chronic stress. Dev Cell. 2007.PMID: 17765679
53. Bernales S. Intracellular signaling by the unfolded protein response.Review Article. Annu Rev Cell Dev Biol. 2006 PMID:16822172
54. Rutkowski DT. Regulation of basal cellular physiology by the homeostatic unfolded protein response. Review Article. J Cell Biol. 2010.PMID: 20513765 PMCID: PMC2878945.
55. Carrasco DR. The differentiation and stress response factor XBP-1 drives multiple myeloma pathogenesis. Cancer Cell. 2007. PMID: 17418411PMCID: PMC1885943
56. Shuda M. Activation of the ATF6, XBP1 and grp78 genes in human hepatocellular carcinoma: a possible involvement of the ER stress pathway in hepatocarcinogenesis. J Hepatol. 2003.PMID: 12713871
57. Luo B. The critical roles of endoplasmic reticulum chaperones and unfolded protein response in tumorigenesis and anticancer therapies. Review Article. Oncogene. 2013.PMID: 22508478PMCID: PMC3819728
58. Greenman C. Patterns of somatic mutation in human cancer genomes. Nature. 2007 PMID: 17344846PMCID: PMC2712719
59. Tameire F et al. TF4 couples MYC-dependent translational activity to bioenergetic demands during tumour progression. Nat Cell Biol. 2019 Jul;21(7):889-899. doi: 10.1038/s41556-019-0347-9. Epub 2019 Jul 1. Erratum in: Nat Cell Biol. 2019 Aug;21(8):1052. PMI:31263264
60. Koumenis C. Regulation of protein synthesis by hypoxia via activation of the endoplasmic reticulum kinase PERK and phosphorylation of the translation initiation factor eIF2alpha. Mol Cell Biol. 2002 PMID: 12370288PMCID: PMC135664
61. Edlund A. A non-glycosylated extracellular superoxide dismutase variant. Biochem J. 1992.PMID: 1463450PMCID: PMC1132032
62. Fujimoto T. Overexpression of human X-box binding protein 1 (XBP-1) in colorectal adenomas and adenocarcinomas. Anticancer Res. 2007.PMID: 17352224

63. Romero-Ramirez L. XBP1 is essential for survival under hypoxic conditions and is required for tumor growth. Cancer Res. 2004.PMID: 15342372
64. Blazanin N. ER stress and distinct outputs of the IRE1α RNase control proliferation and senescence in response to oncogenic Ras. Proc Natl Acad Sci U S A. 2017.PMID: 28847931PMCID: PMC5603998
65. Huang C. Identification of XBP1-u as a novel regulator of the MDM2/p53 axis using an shRNA library. Sci Adv. 2017.PMID: 29057323PMCID: PMC5647124
66. Ghosh R. Transcriptional regulation of VEGF-A by the unfolded protein response pathway. PLoS One. 2010.PMID: 20221394PMCID: PMC2833197
67. Oakes SA. The role of endoplasmic reticulum stress in human pathology. Review Article. Annu Rev Pathol. 2015.PMID: 25387057PMCID: PMC5568783
68. Carrasco DR. The differentiation and stress response factor XBP-1 drives multiple myeloma pathogenesis. Cancer Cell. 2007.PMID: 17418411PMCID: PMC1885943
69. Chapman MA. Initial genome sequencing and analysis of multiple myeloma. Nature. 2011-PMID: 21430775PMCID: PMC3560292
70. Leung-Hagesteijn C. Xbp1s-negative tumor B cells and pre-plasmablasts mediate therapeutic proteasome inhibitor resistance in multiple myeloma. Cancer Cell. 2013.PMID: 24029229PMCID: PMC4118579
71. Oakes SA.The role of endoplasmic reticulum stress in human pathology. Review Article. Annu Rev Pathol. 2015.PMID: 25387057PMCID: PMC5568783
72. Balkwill F. Smoldering and polarized inflammation in the initiation and promotion of malignant disease. Review Article. Cancer Cell. 2005.PMID: 15766659
73. Santofimia-Castaño P et al. Targeting the Stress-Induced Protein NUPR1 to Treat Pancreatic Adenocarcinoma. J.Cells. 2019 Nov 17;8(11). pii: E1453. doi: 10.3390/cells8111453. Review.
74. Vasseur S. p8 is critical for tumour development induced by rasV12 mutated protein and E1A oncogene. EMBO Rep. 2002PMID: 11818333PMCID: PMC1083964
75. Pettersson US. Female mice are protected against high-fat diet induced metabolic syndrome and increase the regulatory T cell population in adipose tissue. PLoS One. 2012PMID: 23049932PMCID: PMC3458106
76. Gräslund S. Protein production and purification. Review Article. Nat Methods. 2008.PMID: 18235434PMCID: PMC3178102
77. Nabarra B et al. Early steps of a thymic tumor in SV40 transgenic mice: hyperplasia of medullary epithelial cells and increased mature thymocyte numbers disturb thymic export. Dev Immunol. 2002. PMID:15144019
78. Reid DW et al. The unfolded protein response triggers selective mRNA release from the endoplasmic reticulum. Cell. 2014 Sep 11;158(6):1362-1374. doi: 10.1016/j.cell.2014.08.012.PMID: 25215492
79. Cinaroglu A et al. Activating transcription factor 6 plays protective and pathological roles in steatosis due to endoplasmi reticulum stress in zebrafish. Author information Hepatology (Baltimore, Md.), 23 Jun 2011, 54(2):495-508 DOI: 10.1002/hep.24396 PMID: 21538441 PMCID: PMC3145024 .
80. Szegezdi E et al. Mediators of endoplasmic reticulum stress-induced apoptosis . EMBO Rep. 2006.PMID:16953201
81. Ohri SS. Inhibition of GADD34, the stress-inducible regulatory subunit of the endoplasmic reticulum stress response, does not enhance functional recovery after spinal cord injury. PLoS One. 2014. PMID: 25386686 PMCID: PMC4227638
82. Chu KY1, et al . ATP-citrate lyase ATP-citrate lyase reduction mediates palmitate-induced apoptosis in pancreatic beta cells. J Biol Chem. 2010 Oct 15;285(42):32606-15. doi: 10.1074/jbc.M110.157172. Epub 2010 Aug 7.
83. Hirsova P1 et al. Lipotoxic lethal and sublethal stress signaling in hepatocytes: relevance to NASH pathogenesis. J Lipid Res. 2016 Oct;57(10): 1758-1770. Epub 2016 Apr 5.
84. Poljsak B et al. Cancer Etiology: A Metabolic Disease Originating from Life's Major Evolutionary Transition? Oxid Med Cell Longev. 2019 Oct 8;2019:7831952. doi: 10.1155/2019/7831952. eCollection 2019.
85. Lee IM et al. Effect of physical inactivity on major non-communicable diseases worldwide: an analysis of burden of disease and life expectancy; Lancet Physical Activity Series Working Group. PMID:22818936
86. Han J Kaufman RJ. The role of ER stress in lipid metabolism and lipotoxicity. J Lipid Res. 2016 Aug;57(8):1329-38. doi: 10.1194/jlr. R067595. Epub 2016 May 4. PMID:27146479.

87. Estébanez B. Endoplasmic Reticulum Unfolded Protein Response, Aging and Exercise: An Update Review. Article. Front Physiol. 2018.PMID: 30568599PMCID: PMC6290262
88. C Dong M . ERdj4 and ERdj5 are required for endoplasmic reticulum-associated protein degradation of misfolded surfactant protein. Mol Biol Cell. 2008 PMID: 18400946PMCID: PMC2397301
89. Zhao L et al. Alteration of the unfolded protein response modifies neurodegeneration in a mouse model of Marinesco-Sjögren syndrome. Hum Mol Genet. 2010 Jan 1;19(1):25-35. doi: 10.1093/hmg/ddp464. PMID: 19801575.
90. Svegliati-Baroni G et al. Lipidomic biomarkers and mechanisms of lipotoxicity in non-alcoholic fatty liver disease. Free Radic Biol Med. 2019 Nov 20;144:293-309. doi: 10.1016/j.freeradbiomed.2019.05.029. Epub 2019 May 29.
91. Eberlé D. SREBP transcription factors: master regulators of lipid homeostasis Review Article. Biochimie. 2004 PMID: 15589694
92. Wang H et al . ER stress and SREBP-1 activation are implicated in beta-cell glucolipotoxicity. J Cell Sci. 2005 Sep 1;118(Pt 17):3905-15. Epub 2005 Aug 9. PMID:16091421
93. Yamashita H et al. A glucose-responsive transcription factor that regulates carbohydrate metabolism in the liver. Proc Natl Acad Sci U S A. 2001 PMID: 11470916 PMCID: PMC55382
94. Mobin MB1 et al. The RNA-binding protein vigilin regulates VLDL secretion through modulation of Apob mRNA translation. Nat Commun. 2016 Sep 26;7:12848. doi: 10.1038/ncomms12848.
95. Libby AE. Perilipin-2 Deletion Impairs Hepatic Lipid Accumulation by Interfering with Sterol Regulatory Element-binding Protein (SREBP) Activation and Altering the Hepatic Lipidome. J Biol Chem. 2016 PMID: 27679530PMCID: PMC5104945
96. Wang LJ1, et al. Betaine attenuates hepatic steatosis by reducing methylation of the MTTP promoter and elevating genomic methylation in mice fed a high-fat diet. J Nutr Biochem. 2014 Mar;25(3):329-36. doi: 10.1016/j.jnutbio.2013.11.007. Epub 2013 Dec 3.
97. Ota T1 et al . Inhibition of apolipoprotein B100 secretion by lipid-induced hepatic endoplasmic reticulum stress in rodents.. Author information. Department of Medicine, Columbia University College of Physicians and Surgeons, New York, New York 10032, USA. J Clin Invest. 2008 Jan;118(1):316-32.
98. Kersten S. et al . Integrated physiology and systems biology of PPARα. Review Article. Mol Metab. 2014 PMID: 24944896 PMCID: PMC4060217.
99. Cho YM1 et al The IRE1α-XBP1s pathway promotes insulin-stimulated glucose uptake in adipocytes by increasing PPARγ activity. Cho YM. Exp Mol Med. 2018 . PMID:30111834.
100. Huang J1 et al. Progressive endoplasmic reticulum stress contributes to hepatocarcinogenesis in fatty acyl-CoA oxidase 1-deficient mice. Am J Pathol. 2011 Aug;179(2):703-13. doi: 10.1016/j.ajpath.2011.04.030. Epub 2011 Jun 12.
101. Kennedy AJ, et al. Mouse models of the metabolic syndrome. Dis Model Mech. 2010 Mar-Apr;3(3-4):156-66. doi: 10.1242/dmm.003467. PMID: 20212084; PMCID: PMC2869491.
102. DeZwaan-McCabe D, et al. ER Stress Inhibits Liver Fatty Acid Oxidation while Unmitigated Stress Leads to Anorexia-Induced Lipolysis and Both Liver and Kidney Steatosis. Cell Rep. 2017 May 30;19(9):1794-1806. doi: 10.1016/j.celrep.2017.05.020. PMID: 28564599; PMCID: PMC5520660.
103. Brown JM, Rudel LL. Stearoyl-coenzyme A desaturase 1 inhibition and the metabolic syndrome: considerations for future drug discovery. Curr Opin Lipidol. 2010 Jun;21(3):192-7. doi: 10.1097/MOL.0b013e32833854ac. PMID: 20216310; PMCID: PMC3099527.
104. Amen OM, et al. Endoplasmic Reticulum Stress Activates Unfolded Protein Response Signaling and Mediates Inflammation, Obesity, and Cardiac Dysfunction: Therapeutic and Molecular Approach. Front Pharmacol. 2019 Sep 10;10:977. doi: 10.3389/fphar.2019.00977. PMID: 31551782; PMCID: PMC6747043.
105. Fafián-Labora et al. FASN activity is important for the initial stages of the induction of senescence. J. Cell Death Dis. 2019. PMID: 30962418PMCID: PMC6453932.
106. Kim YR, et al. Hepatic triglyceride accumulation via endoplasmic reticulum stress-induced SREBP-1 activation is regulated by ceramide synthases.Exp Mol Med. 2019 Nov 1;51(11):129. doi: 10.1038/s12276-019-0340-1.

CHAPTER 7

Scientific Products (bound)

Poster2019 in ERParis2019 congress : NUPR1 orchestrates protein translation during ER-stress by interacting with eukaryotic initiation factor 2α

Borrello Maria Teresa[1], Santofimia-Castano Patricia[1,], Bocchio Marco[2] , **Listi Angela[1]**, Fraunhoffer Nicolas A.[1], Christopher Pin[1], Philippe Soubeyran[1], Eric Chevet[3] and Juan L. Iovanna[1]

[1]Centre de Recherche en Cancérologie de Marseille, INSERM U1068, CNRS UMR 7258, Aix-Marseille Université and Institut Paoli-Calmettes, Parc Scientifique et Technologique de Luminy, 13288 Marseille, France; [2]INMED, INSERM U1249, Parc Scientifique et Technologique de Luminy, 13273 Marseille, France; [3]INSERM U1242, Proteostasis and Cancer Team, Chemistry Oncogenesis Stress Signaling, Université de Rennes 1, Rennes, France. Contact email : maria-teresa.borrello@inserm.fr

American Journal of Physiology Poster Prize (AJP-cell Physiology)